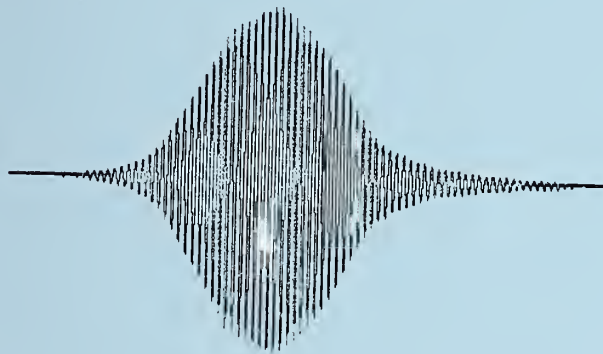


NAT'L INST. OF STAND & TECH
A11106 419362

NIST
PUBLICATIONS

NISTIR 6543

Assessment of Moisture Measurement Techniques for Ceramic Processing



Pu Sen Wang

U.S. DEPARTMENT OF COMMERCE
Technology Administration
Ceramics Division
Materials Science and
Engineering Laboratory
National Institute of Standards
and Technology
Gaithersburg, MD 20899



NIST

National Institute of
Standards and Technology
Technology Administration
U.S. Department of Commerce

QC
100
.U56
NO.6543
2000 c.2

Assessment of Moisture Measurement Techniques for Ceramic Processing

Pu Sen Wang

U.S. DEPARTMENT OF COMMERCE
Technology Administration
Ceramics Division
Materials Science and
Engineering Laboratory
National Institute of Standards
and Technology
Gaithersburg, MD 20899

August 2000



U.S. DEPARTMENT OF COMMERCE
Norman Y. Mineta, Secretary

TECHNOLOGY ADMINISTRATION
Dr. Cheryl L. Shavers, Under Secretary
of Commerce for Technology

NATIONAL INSTITUTE OF STANDARDS
AND TECHNOLOGY
Raymond G. Kammer, Director

Key Words

Moisture measurement techniques; ceramic processing; microwave; near infrared;
nuclear magnetic resonance; magnetic resonance imaging

Cover: Proton free induction decay signal from water molecules.

National Institute of Standards and Technology

NISTIR 6543

Natl. Inst. Stand. Technol.

NISTIR 6543

62 printed pages (August 2000)

**ASSESSMENT OF MOISTURE MEASUREMENT
TECHNIQUES
FOR CERAMIC PROCESSING**

Pu Sen Wang

Ceramics Division

Materials Science and Engineering Laboratory

National Institute of Standards and Technology

Gaithersburg MD 20899

Certain commercial equipment, instruments, or materials are identified in this paper in order to specify adequately the experimental procedure. Such identification does not imply recommendation or endorsement by the National Institute of Standards and Technology, nor does it imply that the materials or equipment identified are necessarily the best available for the purpose.

With Contributions From:

Anthony J. Fanelli
AlliedSignal, Inc.

Ray King
KDC Technology Corporation

Peter H. Krygsman
Bruker Minispec

Gabby Levin
Brimrose Corporation of America

Bob R. Powell
General Motors Corporation

Zeke Seedorff
Pfaltzgraff China

Will Sherratt
Morganite Crucibles

John Szymanski
Zeltex Inc.

TABLE OF CONTENTS

Abstract.....	4
Motivations.....	5
Moisture Measurement Techniques.....	6-8
Microwave Techniques.....	8-13
NMR Spectroscopy and Imaging.....	14-24
Infrared and Near Infrared.....	24-54
Conclusions.....	55
Acknowledgements.....	55
References.....	57-58
List of Figures.....	59-61
List of Tables.....	62

ABSTRACT

This report presents an assessment of moisture measurement tests by techniques currently available for ceramic processing applications. The techniques tested include near infrared, microwave, proton nuclear magnetic resonance, magnetic resonance imaging, and gravimetric methods. The principles of the techniques are briefly described, and the advantages and limitations of the techniques are compared. The forms of the tested samples include powders, pugs, slurries, and greenbodies before and after drying. A near infrared spectrometer can be installed on-line to provide a relatively low cost and simple method. But, it has a limited penetration depth, and the results are influenced by the sample color. While microwave techniques allow for deeper penetration depths with advantages of simple on-line operation and low cost, the high dielectric constant of some materials can complicate the measurement procedure. The emerging NMR and NMR imaging techniques can provide additional information on the physical state of water and its spatial distribution in a ceramic sample. These techniques currently are not widely used due to the high cost, operational complexity and the limitation imposed by the size of the RF-coil. Based on comparisons of performance results, it is suggested that the gravimetric method should be considered as the primary technique for calibration of the other techniques.

1. MOTIVATIONS

Moisture content is a critical parameter in ceramic processing. In the early stages of most ceramic processing, large quantities of water are added to the ceramic powder, binder, and dispersing agents to form a homogeneous slurry. The exact quantity of water added depends on the viscosity desired for the forming technique used. In order to produce homogeneous green parts, a mass fraction of 20 % to 30 % water is quite common.

The green bodies are then dried and fired to form the final products. Drying is often accomplished in an accelerated manner so that the production will be cost effective. A sudden reduction of water in the body can cause a differential volume shrinkage which may result in shape distortion and/or cracking. To assess these effects of drying, both the quantity and the distribution of water over the volume of a green body should be measured, preferably in real time.

Moisture measurement is an important topic receiving close attention by various industries. There have been significant efforts to develop techniques based on specific needs for various products [1, 2]. These products can be liquid, solid, or gas phase. The techniques were developed mainly for the food, pharmaceutical, tobacco, and chemical industries. However, the application of the existing methods to ceramic processing has not been well established. In this report, several techniques such as near infrared (NIR), microwave, proton nuclear magnetic resonance (NMR), magnetic resonance imaging (MRI), and stationary weight loss techniques are evaluated. First, a brief description of the scientific principles of each technique will be presented; then, sample results will be shown to establish the feasibility of each method for application to ceramics. Reference to a well known moisture measurement technique, Karl Fischer titration [3], is also omitted because of its unsuitability for ceramic processing applications.

2. MOISTURE MEASUREMENT TECHNIQUES

Most modern moisture measurement techniques were developed by utilizing the unique physical and chemical properties of water molecules: molecular polarity, O-H bond vibration, and hydrogen nucleus (proton) magnetism. Conventional methods have also been developed for water/moisture determination based on the changes in sample weight, volume, thermal conductivity, density, refractive index, vapor pressure, and other physical properties. Some of these properties, such as volume, vapor pressure, and refractive index, are more sensitive in volatile liquid materials and have only minimal applicability in ceramic processing. Techniques based on other properties, such as thermal conductivity and density, have potential application in ceramics. The most popular techniques in the ceramic industry, however, are the gravimetric methods due to their low cost and ease of operation.

Gravimetric methods basically consider the weight loss in a sample to be related to the moisture content. There are various ways used to remove moisture from a sample: heating at elevated temperature, freeze-drying or desiccation if the sample is unstable at elevated temperatures, desorption of moisture by passing a dry inert gas through the sample, centrifugation, extraction, chromatography, or even forming azeotropes with hydrocarbon or organic halides. The weight measurement and water removal process can be done simultaneously, such as with thermogravimetric analysis (TGA), or they can be in separate stages, such as with conventional oven drying. Figure 1 is a TGA profile at 105 °C of Pfaltzgraff China stoneware clay containing 14 % mass fraction of water. The profile shows that there is an initially fast drying rate followed by a slow rate.

Many ceramic manufacturers currently use only the oven drying technique. This thermal treatment to remove water should not be confused with moisture measurement methods based on thermal property changes, such as thermal conductivity or heat of reaction. With the oven drying technique, it is not always correct to assume that the weight loss due to heating is due solely to moisture content. Several factors need to be considered carefully before the conclusion can be drawn:

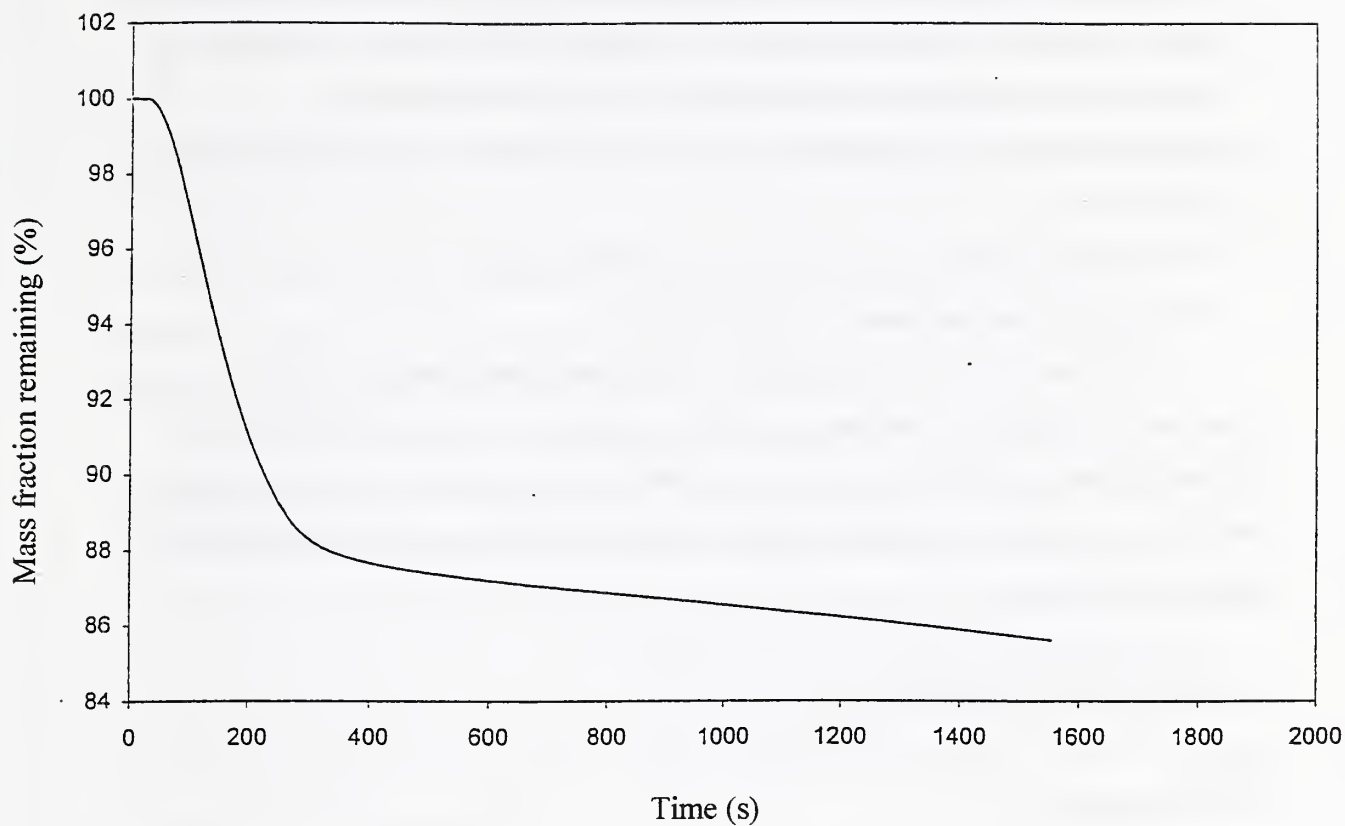


Fig. 1. TGA profile of a stoneware clay sample containing 14 % mass fraction water heated at 105 °C. Note that the profile shows two different drying rates.

1. Choice of heating temperature – A few degrees above the water boiling temperature, 105 °C for example, is often the choice. What are the other components in the sample that will evaporate or decompose at the chosen temperature?
2. Is there any reaction or surface oxidation during heating at a specific temperature for a certain period of thermal treatment? This is particularly important when the ovens used in the ceramic industry are often open to atmospheric conditions.
3. During sample cooling and before weighing, what corrections for surface adsorption are made?
4. Water diffusion behavior and microstructure of the sample – Are there any voids formed due to heating that can entrap moisture?

Oven drying, however, is doubtless the most important primary moisture measurement technique for ceramic processing. It serves as a critical calibration for all other techniques, even though it is destructive and limited by sample size, and cannot be used on-line. All results measured by other techniques in this report are calibrated by the stationary weight loss.

2.1 MICROWAVE TECHNIQUES

2.1.1 Introduction

The O-H bond length in a water molecule is 0.0958 nm and the angle between the two O-H bonds is 104.45°. This bond angle can be formed only with 2s-2p hybrid atomic orbitals from oxygen. The combination of 2s and 2p orbitals forms four sp³ hybrid atomic orbitals for oxygen. Two of the sp³ orbitals are used in O-H bond formation with the 1s atomic orbitals of the hydrogens, and the other two are each occupied by a lone pair of electrons. These lone-pair electrons exert a repulsive force on the bonding electrons changing the bond angle from 109.47°, typical of tetrahedral bonding, to 104.45° [4,5]. This bent molecular structure, with the oxygen end highly rich in electron density, gives the water molecule a dipole moment of 6.17×10⁻³⁰ C·m (1.85 Debye) and a

very large dielectric constant of 78.54 at 25 °C. The lone-pair electrons are also responsible for the hydrogen bonding which is an important property of water.

Several moisture analysis techniques classified as microwave, electrical and electronic methods utilize the high dielectric constant of water molecules that results in a measurable parameter change in electrical or electronic devices, such as electrical capacitance, conductivity, etc. The techniques commonly called “microwave” are most often not classical microwave spectroscopy. Rather, they use a microwave source to measure change of phase, reduction of power, shift of frequency, or reduction in Q-factor of a resonator due to the dielectric constant of water present in the samples. Various types of sensors have been developed for different applications [6,7,8]. The probe can be contact or noncontact, but they are all bulk techniques. There are even imaging techniques developed for mapping moisture distribution [9].

One method involves a noncontact transmission probe. The transmitter and receiver can be either on the same side or opposite sides of the sample. The microwave signal detected by the receiver after passing through the sample is compared with the original microwave signal, and any phase change ($\Delta\phi$ [degree]) or power loss (ΔA [dB]) due to the sample is detected. The transmitter also can be designed to function as the receiver [6]. In this case, a reflector is required on the opposite side of the sample to backscatter the microwave radiation to the transmitter/receiver. Figure 2 shows the design of such a two-way transmission.

In either case, the mass fraction of moisture content (w_m) can be determined with a quadratic model:

$$w_m = K_0 + K_1X + K_2X^2 \quad (1)$$

where the K_i 's are calibration constants for the microwave method and $X = (\Delta A - A_0)/(\Delta\phi - \phi_0)$. With proper choice of A_0 and ϕ_0 , this model generally can be constructed to be independent of the thickness or density of the test material.

A second method uses a contacting open reflection resonator sensor that is configured so that the electromagnetic fields fringe into the test material thereby affecting

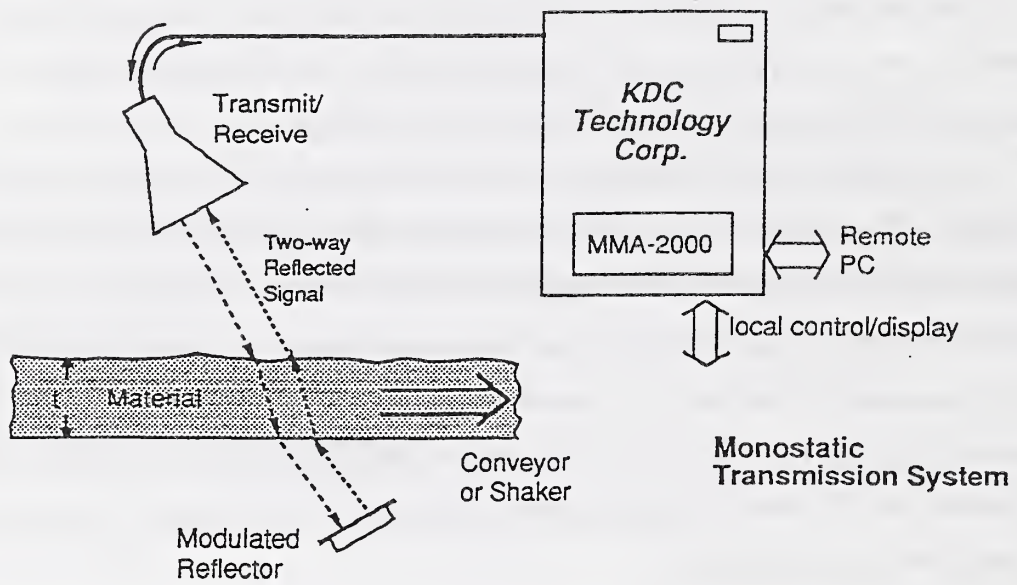


Fig. 2. The design of a two-way transmission microwave system for moisture measurement. (Reproduced with permission from R. J. King of KDC Technology).

the sensor's resonant frequency (f_r) and input resistance (R_O) at resonance. These two raw measured parameters are inversely related to the dielectric constant (ϵ') and loss factor (ϵ'') of the test material, respectively. Then w_m is determined using the same quadratic form given in Eq. (1), but in this instance $X = (\epsilon'' - \epsilon''_0) / (\epsilon' - \epsilon'_0)$, and $\epsilon'_0, \epsilon''_0$ are calibration constants that are chosen to make Eq. (1) independent of material density.

2.1.2 Experimental

Two (2) specimens, stored separately in plastic bags, labeled “A” and “B” were measured with a hand-held open resonator sensor manufactured by KDC Technology Corporation, Livermore, California. Both specimens contained nominally the same ceramic composition of aluminosilicate/ graphite/ silicon carbide mixture provided by Morganite Crucible. The specimens were small, soft and irregular in shape. Because they contained a high percent of graphite which shows a total photo-absorption, microwave would be a better choice over the infrared or near infrared technique.

Specimen A was used as the control. A's moisture mass fraction content was measured gravimetrically as 13.2 %. Microwave data were taken using a hand-held probe applied to four different locations on the specimen, reading from outside its plastic bag. A was left in its bag for three days, then measured gravimetrically again at 13.0 % mass fraction of moisture, indicating 0.2 % loss during storage. Using the resonant frequency as the indicator of moisture content, the microwave probe reading had changed by 0.32 %. The small discrepancy (0.32 % versus 0.2 %) is attributed to random variations in specimen composition, texture and thickness, combined with the effect of the edges of the small specimens and the presence of the plastic bags, and variation in hand pressure. The standard deviation of the four different readings was about 4 MHz or 0.35 % mass fraction in moisture content, which is rather high for this technique.

Specimen B was used to test the sensitivity of the microwave probe. B's initial moisture was measured gravimetrically as 17.7 % mass fraction. As for specimen A, microwave data were taken at four different locations. B was then dried for two hours, returned to its bag for three days to equilibrate, then measured gravimetrically again. The

second determination was 13.6 % mass fraction in moisture. The microwave probe reading changed by 46 MHz, equivalent to a change of 11.2 MHz per percent change in moisture content. The resolution of the technique is 100 KHz or a factor of 1/100 of one percent. The standard deviation of the four different readings was in each case about 4 MHz, or 0.35 % mass fraction in moisture content, probably for the same reasons given above. This deviation is expected to fall dramatically for larger sample sizes, larger specimen sizes, and using automated data collection with sensors developed especially for this soft crumbly material.

2.1.3 Results and Discussion

These resonant sensors can have many forms, shapes and sizes that are appropriate to the material form (liquid, powder, particulate or solid), moisture range and on-line, hand-held or bench instrument application (Fig. 3). Compared to the (non-contacting) one or two-way through transmission methods, the (contacting) resonant sensor method offers the best sensitivity and resolution to small changes in moisture, particularly at low (< 20%) levels [8]. In both methods, the bulk w_m is measured. This indicates that the technique is sensitive enough to measure the moisture content in a drying experiment. Figure 3 shows such an experiment by plotting moisture content vs. drying time in open air for a green ceramic feedstock. It is obvious that the technique has sufficient sensitivity for moisture removal processing as low as $dw_m/dt = 0.002\% / \text{min}$.

The microwave method is a low cost, simple to operate bulk technique that can be installed on-line. However, the measurement principle is based on the large dielectric constant of water molecules. In a sample containing a component with a dielectric constant comparable to that of a water molecule, the contribution from this component should be separated from that of moisture in order to obtain an accurate result.

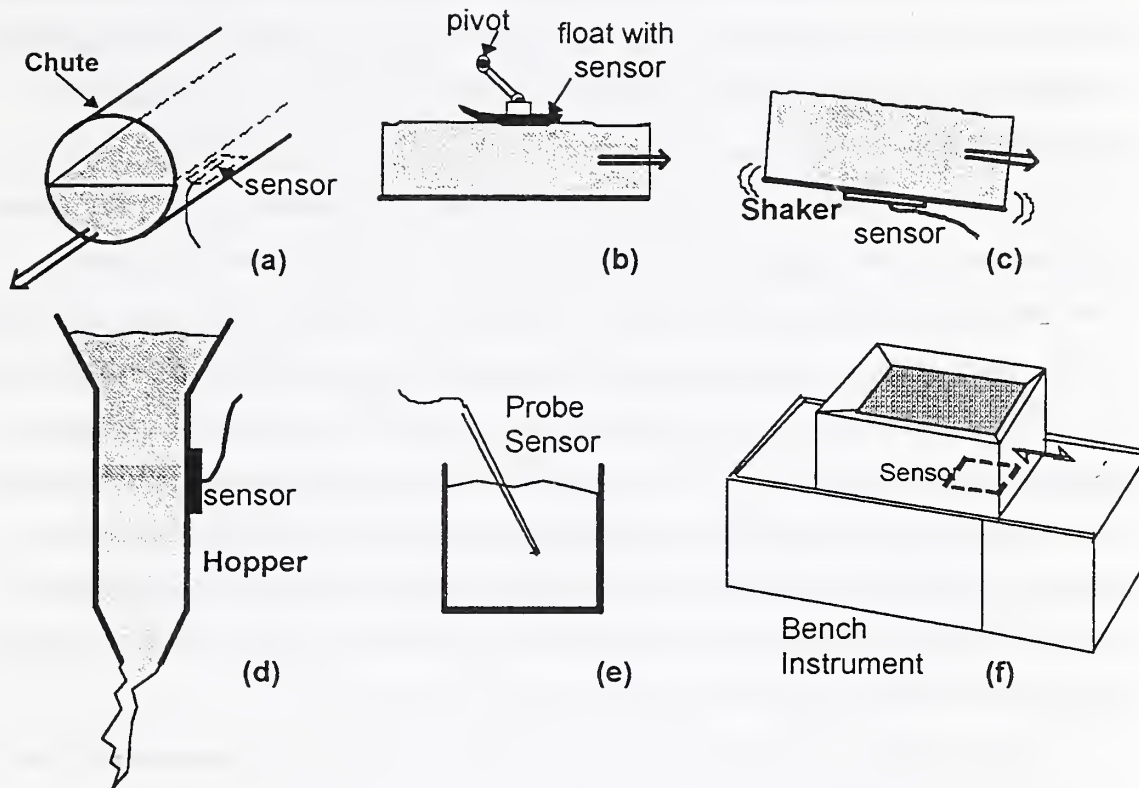


Fig. 3. Typical applications of microwave resonator moisture sensors (Reproduced with permission from R. J. King of KDC Technology).

2.2 NMR SPECTROSCOPY AND IMAGING

2.2.1 Introduction

Spectroscopic methods for water/moisture measurement are starting to be used for monitoring ceramic processing. These techniques initially require relatively large efforts in training and capital investment. Due to the rapid growth in personal computer and electronic technology, however, they are now easier to operate, nondestructive, and sometimes on-line. More importantly, these advanced spectroscopic methods can provide information at the molecular level that other methods cannot. The methods cover a complete range of energy absorption from water molecular electron excitation, OH bond vibration and rotation, to proton magnetic resonance. Namely, they include ultraviolet (UV), visible (colorimetry), infrared (IR), near infrared (NIR), and nuclear magnetic resonance (NMR). Analysis by UV and colorimetry requires additives such as potassium dichromate and cobaltous chloride, respectively, to induce UV absorption and color change. The addition of additives contaminates the samples making these methods less attractive. NMR, IR, and NIR are becoming the most interesting spectroscopic techniques currently used for moisture measurement in ceramic processing.

The association and interaction of water with materials is very complex and not well understood. Pauling defines “crystallization water” as water accompanying a chemical compound when crystallized from an aqueous solution, while “constituent water” is the water that will change the chemical nature of a compound when it is lost [10]. For simplicity in understanding water behavior in ceramic processing, water molecules in the liquid state can be classified into three types: bulk water, surface adsorbed water, and bound water. The molecules of the bulk water are far enough from the ceramic particulates (or other solids such as binders, sintering aids, etc.) that there are no interactions between them. In the second category are water molecules that are adsorbed on the solid surface. They lose a certain degree of molecular freedom due to the physical bonding of the molecules to the solid surface. The “bound water” consists of molecules that have been trapped in small voids such as interstices and vacancies in the crystal lattice, interlayer regions of clay, or the cavities formed by the arrangement of

ceramic particles. The molecular dynamic degrees of freedom in this case may be greater than those of the surface adsorbed water, but less than those of the bulk water. The molecular kinetic energy is different for each state of water, and the energy required to remove the water is also different for each state. Modern spectroscopic techniques can differentiate among the different states and, therefore, can enhance the understanding of ceramic processing technology. NMR spectroscopy is such a technique.

Each water molecule has two hydrogens and each hydrogen has a proton with a nuclear spin number, I , of $\frac{1}{2}$. The possible number of orientations of its magnetic moment with respect to the direction of an applied external magnetic field is $(2I+1)=2$. The component of the nuclear spin moment along the external magnetic field can be either $+\frac{1}{2}$ (spin up state, excited state) or $-\frac{1}{2}$ (spin down state, or ground state). The energy difference between the two states falls in the radio frequency (RF) region of the electromagnetic spectrum. For example, at a field of 9.4 T, the energy difference corresponds to a RF frequency of ~ 400 MHz. If a wet ceramic sample is placed in such a magnetic field and irradiated by such a frequency, some of the protons from water molecules will be excited from the ground state to the excited state by absorbing the RF energy. Figure 4 shows a proton energy level, E , split by the presence of an external magnetic field, B_0 and Figure 5 is a block diagram of a NMR spectrometer with imaging facility. Note that in Figure 4, the number of the excited protons (or the intensity of the absorption spectrum) is directly proportional to the amount of water in the sample. Comparisons of absorption intensities provide a technique for moisture measurement in ceramic samples.

Figure 4 also shows that the protons in the excited state are unstable and will return to the ground state by releasing the absorbed RF energy. In “free tumbling” water, molecules have a larger kinetic energy and collide with neighboring molecules frequently. This provides an excellent path to release the RF energy to the crystal lattice and the time constant required for nuclei in the excited state to return to the ground state through transferring the RF energy to the crystal lattice is designated as T_1 (nuclear spin-crystal lattice relaxation time). By comparison, in a solid sample, the molecules are less dynamic, more rigid, and a strong dipole-dipole interaction occurs between two neighboring spin centers. This nuclear spin-spin interaction thus replaces the nuclear

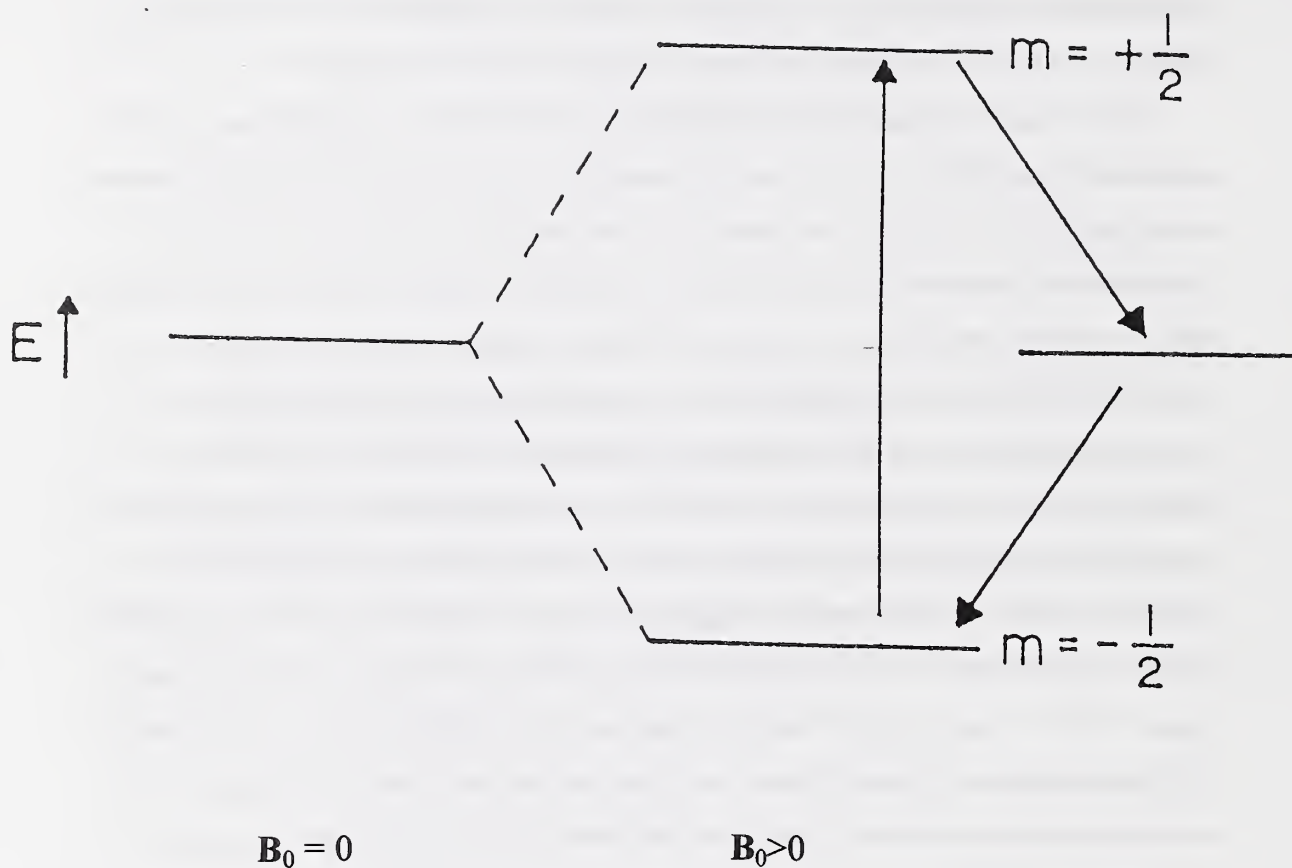


Fig. 4. Nuclear energy levels of a proton in an external magnetic field. There are two relaxation mechanisms, nuclear spin-spin or nuclear spin-crystal lattice, when it returns from the excited state to ground state.

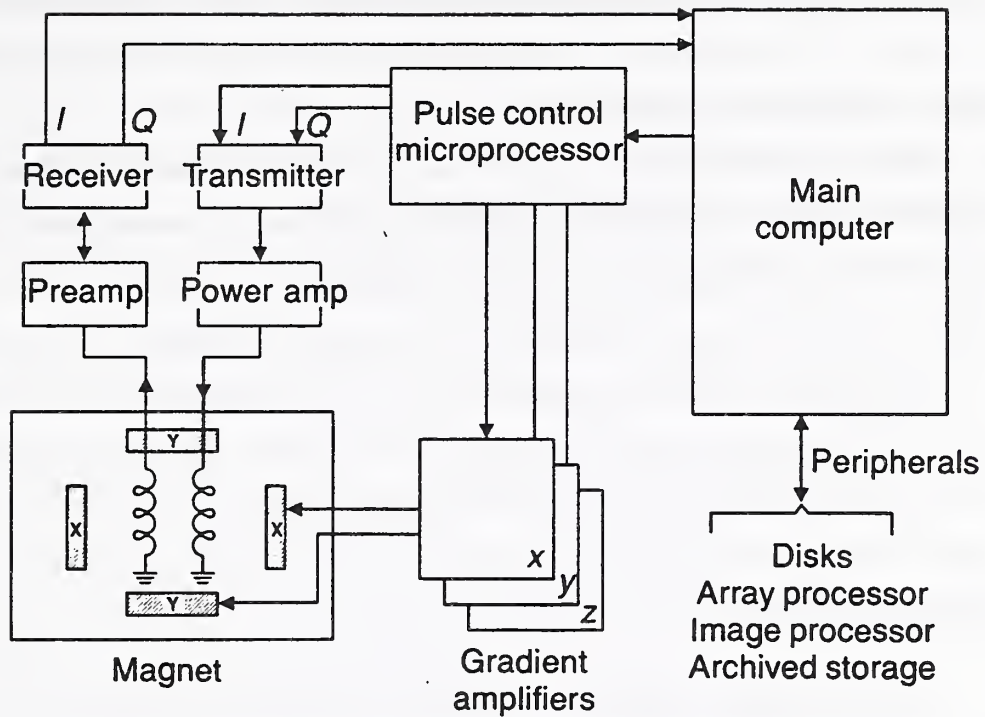


Fig. 5. A block diagram of a NMR spectrometer with imaging capability. The gradient coil is used to convert a spectroscopic signal to a spatially resolved picture.

spin-crystal lattice to be a more effective path for energy release; and the time required to complete the process of returning from the excited state to the ground state through this path is characterized by T_2 (nuclear spin-spin relaxation time). In short, a mobile water molecule has long T_2 and short T_1 while a rigid molecule (such as from the ice) has long T_1 and short T_2 . Thus, the relative T_2 value can provide information on the physical state of water molecules in a ceramic sample.

There are two techniques for measuring T_2 values. Since a solid sample gives a broad NMR signal and represents a strong dipole-dipole interaction with short T_2 , then T_2 must be inversely proportional to the NMR linewidth:

$$T_2 \sim (\Delta H_{1/2})^{-1}$$

where $\Delta H_{1/2}$ is the linewidth at half-maximum intensity [11].

2.2.2 Experimental

The ceramic green compacts were molded by AlliedSignal proprietarily. The injection molding feedstock was made from β -spodumene powder (roughly 85% $\text{LiAlSiO}_4/15\% \text{SiO}_2$), water, dispersant, and agar powder. The materials were combined in a heated sigma blender to a dough-like consistency. After cooling, the material was removed from the blender and shredded into particulate suitable for feeding into the hopper of an injection molding machine. The mass fraction of solids in the feedstock is 73.4 %.

Molding was carried out in a Boy 15S press, equipped with a special alloy CM 9V barrel and screw to minimize metal contamination. Three zone heaters along the barrel provided a temperature profile of 83 °C, 82 °C, 50 °C from the nozzle to the feeding throat of the injection molding machine. The die was maintained at 23 °C. A normal molding pressure (hydraulic) of 2.8 MPa (400 psi) was used for a part of a C-clamp weighing 23 g. The parts were cut to fit into 20 mm NMR tubes and sealed to avoid drying.

The NMR imaging facility consists of a Bruker MSL-400 system with a selective excitation unit, a micro-imaging probe, a gradient drive unit, a low power (5 watts) linear amplifier, and other accessories. The RF frequency for ^1H resonance was 400.159972 ± 0.000001 MHz. A 20 mm diameter RF-coil insert was used for sample mapping.

The pulse sequence used to acquire echo signals, phase encoding, and T_2 -weighting for image construction is $D_0-(\pi/2)_{\pm x}-\tau-D_{10}-D_7-(\pi)_x-D_7-D_{10}-AQ-D_0$ where τ is the variable delay between the 90° and 180° pulses in Hahn's echo detection sequence and which is also used here for phase encoding time, AQ is the echo acquisition time and D_{10} and D_7 are delays for T_2 -weighting and gradient coil stabilization, respectively. D_0 is a long delay (20 s in our experiments) for the bulk nuclear magnetization to reach the spin temperature equilibrium. A maximum field gradient of approximately 6×10^{-3} T/cm was generated for phase encoding.

The $\pi/2$ pulse width was $19.5 \mu\text{s}$ in the spin echo sequence for imaging "bound" water. But for the "free" water, a "soft" pulse of sinc shape replaced the "hard" pulse to avoid diffusion. The detail can be found elsewhere [12-13].

2.2.3 Results and Discussion

Figure 6 represents a set of Fourier-transformed proton free induction decay signals from a wet clay sample heated at 105°C . The top signal is from a green body with a crack which created a large void filled with "free-tumbling water" (the sharp tip with linewidth ~ 500 Hz on the peak). The second signal from the top represents an unheated greenbody without cracks so that no such sharp tip from the "free-tumbling water" can be observed. Since this wet sample contains 18.4 % moisture, the majority of the water molecules are "mobile" and a linewidth of ~ 5500 Hz was observed. As the heating went on, the "mobile water" continued evaporating, and an increase in linewidth can be observed. After 39 min at 105°C , all mobile water was evaporated and only surface absorbed water remained in the sample. A broader line of width ~ 10000 Hz was detected that represents this physically bound water. After 63 min, all water (mobile and physically bound) has been removed and a broad line of ~ 18000 Hz was observed. This

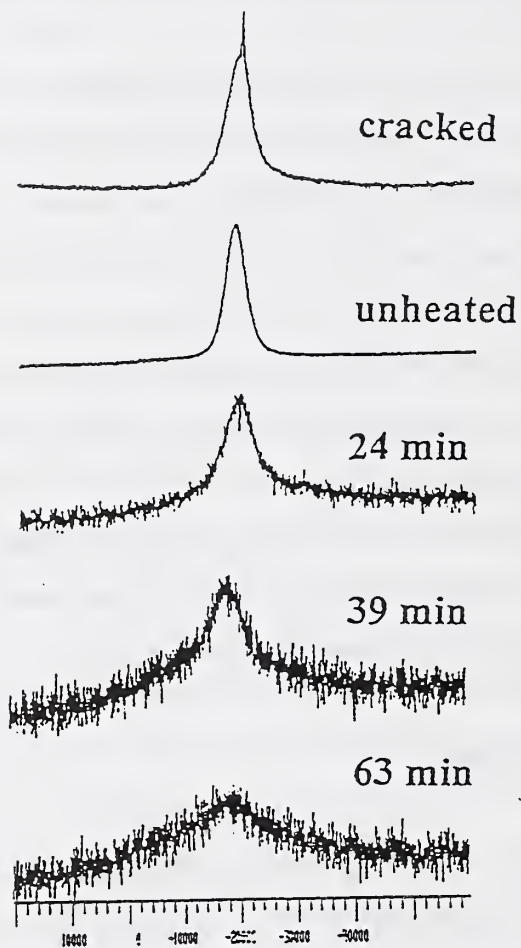


Fig. 6. NMR lineshapes of a clay sample containing, from top to bottom, unheated sample with crack, unheated without crack, heated at 105 ° C for 24 min., heated at 105 ° C for 39 min, and after 63 min heating, all moisture was removed and the broad line is due to Al(OH)₃. Note that “free water” accumulated in the crack and has a much narrower linewidth because of molecular tumbling (top curve).

broad line is due to the protons of $\text{Al}(\text{OH})_3$ which is part of the clay and cannot be removed at 105 °C. This set of data shows clearly the power of NMR to identify the state of water molecules that other techniques cannot achieve.

An alternate way of measuring T_2 is by nuclear spin-echo multiple pulse sequence [12]. T_2 can be calculated from

$$I = I_0 \exp(-t/T_2) \quad (2)$$

where I and I_0 are the nuclear echo signal intensities at time t and at equilibrium, respectively. Figure 7 shows a nuclear spin-echo intensity decay of moisture in an alumina sample. The fast decay represents “bound water” (shorter T_2 , 14.2 %) while the slow decay region is due to “free water” (longer T_2 , 16.8 %). Bound water is strongly associated with solid materials so that reorientation and molecular motion is relatively restricted and therefore slow on an NMR timescale. Bound water does not necessarily include all water trapped in a pore or cavity since the size of the cavity may be large enough to contain a pool of free water. Here bound water is considered trapped water, but trapped water is not necessarily bound from the point of view of NMR spectroscopy. Figure 7 indicates that the fast decay component is associated with the bound water, and the slow decay component is free. Note that in the present study T_2 is just a relative number and has no absolute meaning as some instrumental parameters can contribute to its value. It is the relative linewidths (or echo intensity decay rates) from a sample containing multiple signal line shapes that reveal the physical state of moisture in this sample.

Economical benchtop NMR analyzers are available for routine analysis of moisture content in samples that can fit into the sample compartment. Maximum size is limited by the magnet airgap and the nature of the experiment. Currently, the maximum size is 30 mm for determination of bound and free water, and up to 50 mm if free water only is to be determined. The cost of the equipment depends on the number of detectable nuclei and other functions of the spectrometer desired. Benchtop low resolution NMR yields information about the state of water and quantity of water – total amount and amount in each of the states (e.g. free and bound).

A new NMR device is available that can sample on and beneath the surface of an object. The magnet and RF coil is hand-held and connected to the rest of the analyzer by a flexible cable. The device, called the NMR MOUSE, is currently used to characterize the environment of

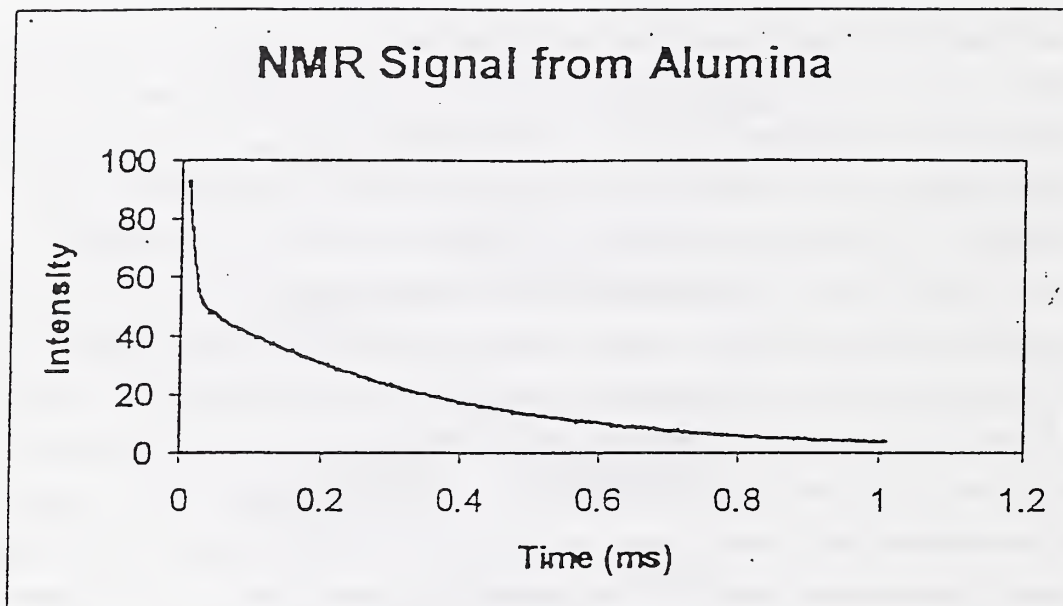


Fig. 7. Nuclear spin-echo intensity decay of moisture from an Alumina sample. The fast decay region represents bound water (14.2 %) while the slow decay region is due to free water (16.8 %). (Data from Bruker Minispec).

hydrogen in rubber. New developments underway may soon make the device appropriate for quantitative moisture determination on and near surfaces of objects like green bodies.

An emerging technology for internal mapping is NMR imaging, or MRI, magnetic resonance imaging, as more often applied in medical science. As can be seen from Figure 5, an NMR imaging facility consists of an NMR spectrometer plus field gradient accessories – RF pulse generators, pulse shapers, three power amplifiers (audio frequency), and a set of gradient coils to generate field gradients along the x, y, and z axes. The function of the field gradient is to convert the spectroscopic intensities to a spatially resolved picture. Several different types of NMR mapping can be obtained. Depending on the technical information desired, these types can be generated by spectroscopy – T_1 , T_2 , or chemical shift, etc. T_2 -weighted mapping has been the most popular technique because:

1. Short data acquisition time – T_2 values are typically very small, in the range of microseconds or milliseconds.
2. It differentiates solid (a tumor) from liquid (a cyst) readily – A medical diagnosis of internal tissues requires only a few minutes without surgery, by changing “echo time” and comparing picture intensities.

The application of NMR imaging in ceramics is still in its infancy. The reasons are both economical and technical. The cost of the facility is relatively high and ceramics are hard solid materials. The hardness of ceramics requires a train of power amplifiers to generate sufficient power output for the RF-pulses. The extremely broad lineshape due to strong dipole-dipole interactions results in a very short T_2 value that challenges the limits of the time-constant of electronic components. The facility at NIST is capable of performing solid imaging at the proton frequency. Solid organic binder (a wax/polypropylene mixture) distributions in injection molded alumina greenbodies have been studied by monitoring nuclear spin-echo intensities [13]. Silicon nitride slurry homogeneity has also been investigated by a “soft pulse technique” to map the water distribution in the slurries [14]. We have even developed a mapping technique by using magnetic stray-field, rather than gradient coils, combined with a “solid echo” pulse sequence to study the distribution of polyethylene glycol (PEG) in silicon nitride greenbodies [15]. An example of water distribution in green ceramic is presented in

Figure 8. The water is in a gel form in the presence of agarose, which functions as a binder. The figure is a slice of 64 2D images lying along the XY-plane that can be used to construct a 3D image, showing several internal defect points (darker points) containing high water contents in this green ceramic sample. These points will be weak spots with lower density after firing. It is also possible to quantify any point defect by intensity profiling along a column or a row containing this point.

This technology, however, has the disadvantages of high cost, size of the sample limited by the RF-coil, and reduction and distortion of sensitivity by metallic impurities presented in the sample. A NMR spectrometer with an open RF-coil is currently under development by Bruker Instruments for material characterization.

2.3 INFRARED (IR) AND NEAR INFRARED (NIR)

2.3.1 Introduction

A water molecule has three atoms and thus nine degrees of freedom for each molecule. Since it is a bent molecule having three rotational modes, there are only three modes that can be assigned to the fundamental molecular vibrations after three degrees of freedom of translational motions are subtracted. Each of these three vibration modes possesses its characteristic energy and symmetry, and are described as “symmetric stretching”, “scissoring”, and “asymmetric stretching” [16]. Figure 9 shows the modes of these vibrational motions and the frequency of the vibration, ν (in cm^{-1}), can be calculated from

$$\nu = (2\pi c)^{-1} \{ \kappa [M_x M_y / (M_x + M_y)]^{-1} \}^{1/2} \quad (3)$$

where c is the speed of light, κ is the force constant, and M_x and M_y are the mass of atoms x and y , respectively. When a light beam impinges on the surface of a sample containing moisture, the photo-energy corresponding to the characteristic energy of these vibration modes will be absorbed. The photo-intensity loss at these frequencies can be used to quantify the concentration of moisture present in the sample. Figure 10 shows a simple diagram of such an infrared spectrometer for moisture measurement in reflecting mode.

BRUKER NMR

25-02-97

309



1

Fig. 8. A slice from a 3D NMR image, showing internal defect points detected in a green ceramic sample. The spots with high intensity will be weak points after firing.

Symmetric
Stretching

3652 cm^{-1}



scissoring

1595 cm^{-1}



asymmetric
stretching

3756 cm^{-1}

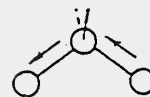


Fig. 9. Molecular vibration modes of a water molecules. They are, from left to right, symmetric stretching, "scissoring", and asymmetric stretching, respectively.

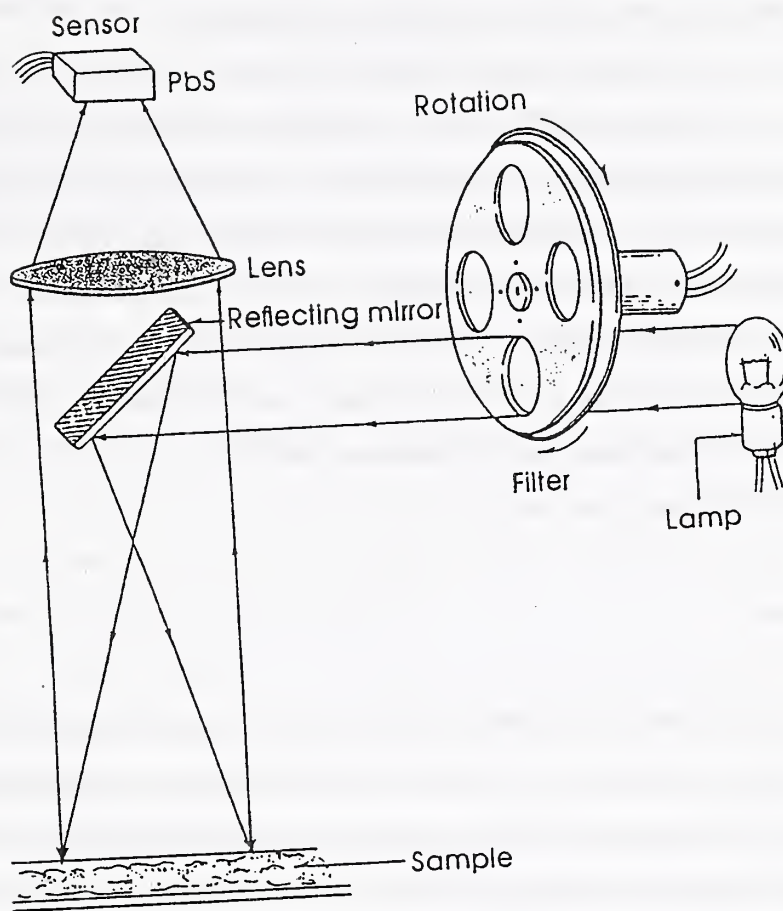


Fig. 10. A block diagram of an IR (or NIR) spectrometer. The difference between the two lies in the frequency region of detection. NIR penetrates deeper into the sample. (Reproduced from Zeltex's literature with permission).

Note that a transmission mode can also be used if the sample is thin and transparent. The characteristic frequencies for these three vibration modes are in the infrared (IR) regions of 3652 cm^{-1} , 1595 cm^{-1} , and 3756 cm^{-1} for the symmetric stretching, “scissoring”, and asymmetric stretching, respectively. The chemical and physical environment of water molecules in the sample may shift these frequencies considerably.

IR analysis of ceramic samples shows various degrees of surface effects since most ceramic samples are not transparent. There is also a problem with detector saturation because of the strong absorption by the water molecules. A way to circumvent these problems is to measure the signals detected in the higher energy range of the overtones and combinations of these fundamental frequencies. These signals fall into the NIR range which can detect several millimeters into the sample surface, while IR can measure only to depths of less than a millimeter. For measuring water, the first overtone of the 3652 cm^{-1} signal at $\sim 7300\text{ cm}^{-1}$ and the combination of the 3652 cm^{-1} and 1595 cm^{-1} modes at $\sim 5250\text{ cm}^{-1}$ are most often used.

2.3.2 Experimental

In the slurry drying and percent solid studies, the spectrometer used was a Luminar 2030 model by Brimrose Corporation of America and the samples were supplied by General Motors (GM) Corporation. The on-line moisture measurements were performed in the Pfaltzgraff production line with a Zeltex, Inc. KJT 100 Moisture Analyzer. The powder moisture was measured by a KJT 200 model and the powders were supplied by NIST.

In the slurry drying and percent solid studies, a sample from the same source was used to collect a spectrum labeled as zero dilution. Water was added to each bottle in varying quantities, from 3 mL to 10 mL. After each addition, the sample was weighed again, shaken well, and a sample was drawn to collect the spectrum. The bottle was weighed again, and the new weight was used to calculate the next value of the percent solids (PS).

Five samples were taken from five of the bottles, and each one placed in a small aluminum foil cup. These were weighed, a spectrum was collected, and then the cups were placed in an oven at $43\text{ }^{\circ}\text{C}$ ($110\text{ }^{\circ}\text{F}$). After about 10 min, the samples were removed,

weighed, and their spectra were collected again. This created samples with higher PS values.

The intention of the drying experiments was to see if the spectrometer can follow the drying of a sample in real time, from which rates can be deduced by following the time intervals at which the spectra are collected. For the purpose of this test, four samples of foamed polystyrene were partially coated by immersion in the experimental casting slurry. They were weighed, a spectrum was collected, then were allowed to dry in free air in the room. After several minutes, the samples were weighed again, and the spectrum was collected again. The drying period was gradually increased, as we suspected a decrease in drying rate. The spectrum of the polystyrene was collected for use as a background if necessary. Ten samples of slurry taken from the experimental casting line were allowed to evaporate water, so as to achieve variations in initial percent solids. These were then used to create additional variability by adding water and also by accelerated drying in an oven. The PS was determined by using the standard procedure at GM, i.e., weighing before and after drying in an oven. This is a basic procedure, and is often referred to as loss on drying (LOD).

For the dilution experiment, a sample of about 360 g was placed in a bottle and a Luminar 2030 spectrometer with a beam area of about 6 mm x4 mm was used. It is estimated that such an area will be useful in actual measurements on parts such cups and handles. The sample was placed on a stage at a distance of 40 mm from the front window of the optical module. Since rotation of the actual hardware during the measurement is not realistic, it was decided to examine the quality of the results without rotating the samples. It was estimated that since the particle size of the powder is so fine, the beam area is sufficient to average the reflectance from a large enough number of particles, providing sufficient averaging to allow the sample to be static. The spectral range was 1200-2200 nm. Scanning was done at a rate of $\sim 16,000 \text{ cm}^{-1}/\text{s}$. At this rate it is possible to scan the desired range at a rate of ~ 30 scans per second. Thus, collecting 200 scans is only a matter of ~ 7 s. In actual production, once a robust calibration curve is established, it is possible to use 60 scans or so, and this will require only 2 s. Each spectrum consists of 200 scans that are averaged into one spectrum. The data was collected in the transmission mode, without any background correction, and post processed into

absorption. Since each dish started with different initial % moisture, and since the time intervals were not identical, each sample yielded different % values during the experiment, increasing the effective number of data points significantly. The data for each dish were collected in different files, which were later merged into one file.

The procedure used for calibrating the Zeltex, Inc. KJT 100/200 Moisture Analyzers for testing ceramic materials was as follows:

Samples of silicon nitride, aluminum oxide, zirconia/yttria, and aluminum nitride II were hydrated in a humidity chamber for from 5 min to 60 min. All samples were allowed to stabilize in sealed containers overnight. The ceramic samples were dried in a forced air oven at 130 °C. and weighed at different time intervals to determine the moisture loss compared to the dry mass of the material.

The calibration set was developed by comparing the absorbance numbers that were generated by the KJT-200 Moisture Analyzer to the percentage of moisture values that were calculated from the moisture mass loss ratios from each ceramic powder sample. The computed moisture and absorbance values were typed into the analyzer to obtain a statistical regression analysis of the moisture calibration using the analyzer's own regression routines.

Firmware in the desk-top instrument KJT-200 Moisture Analyzer computes a line of best fit through the data points using a linear ($Y = A_0 + A_1 X$), quadratic ($Y = A_0 + A_1 X + A_2 X^2$), or cubic curve fit ($Y = A_0 + A_1 X + A_2 X^2 + A_3 X^3$) to determine the best measurement standard error (SE). The measurement constants for each material can be stored in the analyzer and up to 50 separate calibrations may be saved in this device. The same procedure is used for calibrating the KJT-100 Portable NIR Moisture Analyzer.

2.3.3 Results and Discussion

The results of the weight loss vs. time presented as PS are given in Table 1. An initial value of 43.00 % was used. Fig. 11 shows an example of a sequence of NIR spectra of water in a ceramic slurry during a drying experiment. The top spectrum represents the starting slurry which contains 61 % mass fraction water. The peaks at 1460 nm ($\sim 7300 \text{ cm}^{-1}$, first overtone of symmetric stretching) and 1940 nm ($\sim 5250 \text{ cm}^{-1}$,

Sample:	1		2		3		4	
	Clock time	Solids %	Clock time	Solids %	Clock time	Solids %	Clock time	Solids %
	8:32	43.00	8:32	43.00	8:33	43.00	8:33	43.00
	8:41	44.60	8:36	44.10	8:39	44.30	8:37	44.00
	8:47	45.75	8:43	45.22	8:46	45.60	8:44	45.14
	8:57	47.45	8:49	46.66	8:55	47.35	8:51	46.44
	9:07	49.42	8:58	48.35	8:55	49.35	8:51	48.14
	9:21	52.30	9:12	51.06	9:18	52.00	9:13	51.04
	9:35	53.67	9:25	54.25	9:31	55.33	9:27	54.28
	9:57	60.92	9:48	59.00	9:52	59.40	9:50	59.20
	10:21	64.10	10:11	61.60	10:17	61.73	10:14	61.32

Table 1. Mass fraction of solids as a function of drying time in air, based on weighing samples of the coating on a foamed polystyrene sample. The uncertainties are ± 0.02 %.

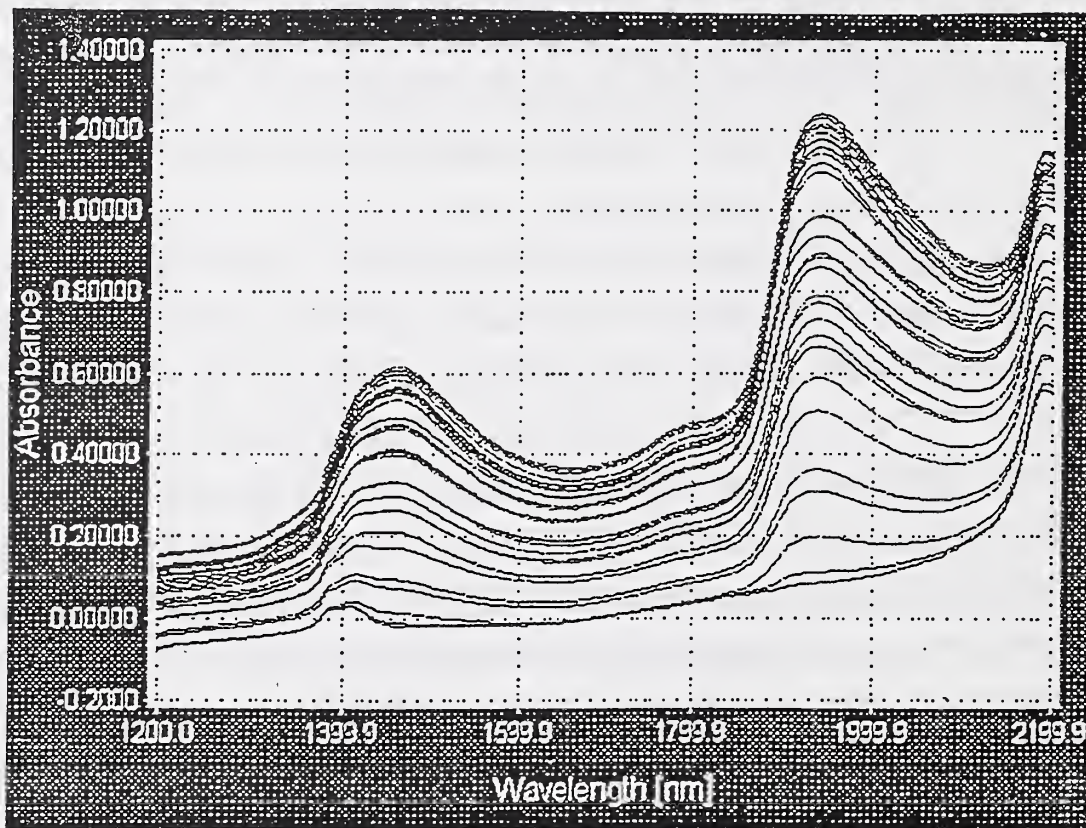


Fig. 11. A sequence of water NIR spectra from a slurry containing ~60 % mass fraction of water during drying. The peak at ~1460 nm ($\sim 7300 \text{ cm}^{-1}$) is the first overtone of 3652 cm^{-1} (O-H symmetric stretching from water molecules). The ~1940 nm ($\sim 5250 \text{ cm}^{-1}$) peak is from the combination of 3652 cm^{-1} and 1595 cm^{-1} “scissoring”. Note the weak ~1400 nm peak remains even when the sample is dry. (Data supplied by Brimrose Corporation of America and General Motors Corporation).

combination of symmetric stretching and scissoring) are very clear. As drying at 43 °C (110 °F) goes on, the intensity decreases at these two peaks. When the slurry is completely dry, the 1940 nm peak disappears completely, as expected. However, a weak peak remains in the ~1400 nm region (bottom spectrum). This 1400 nm peak can be due to other O-H bonds from the native surface oxide film on ceramic powders in the slurry, or formation of chemically or physically bound water that cannot be removed at 43 °C. Not all spectrometers have this capability to achieve detection of this additional information. It depends on the design, sensitivity, quality, and thus cost of the spectrometer. Often, taking the derivative of an absorption spectrum, which indicates the change of curvature, will give additional complex technical information. Figure 12 shows the 2nd derivatives of the spectra in Figure 11. The decrease in intensities is once again observed during drying. In addition, more structure was resolved which suggests additional information about the slurry. In order to extract the information, other experiments have to be performed. The picture revealed that a full spectrum holds much more information than a spectrum based on discrete wavelengths, as is the case for spectrometers based on filters.

We can deduce from the spectrum that the large absorptions in the 1410 nm and 1900 nm regions are definitely associated with absorption of water. Other absorptions can be possibly linked with the solids, or maybe with other constituents in the slurry. It is very important to pay attention to the spectral region around 1380 nm to 1460 nm. When the water level is still high, the peaks at 1460 nm and 1940 nm are dominant, and the situation is clear. As water disappears, the peak at 1940 nm is almost completely gone, and so is the peak at ~1450 nm. However, the peak around 1380 nm to 1410 nm does not diminish in the same way. This is important, as it is probably associated with the solids. If so, it can be an important area in determination of PS.

Figure 13 is a set of NIR spectra from clay samples containing up to ~31 % mass fraction of water. Dry powder samples were also tested. The ~1400 nm “bound water” observed previously in the slurry sample is very strong in these dry powders. It is so because clay contains large amount of $\text{Al}(\text{OH})_3$ which can only be decomposed above 500 °C [17]. Table 2 includes the data from three runs, with water content ranging from ~15 % to 30 % mass fraction. The removal of the three outliers improves the calibration

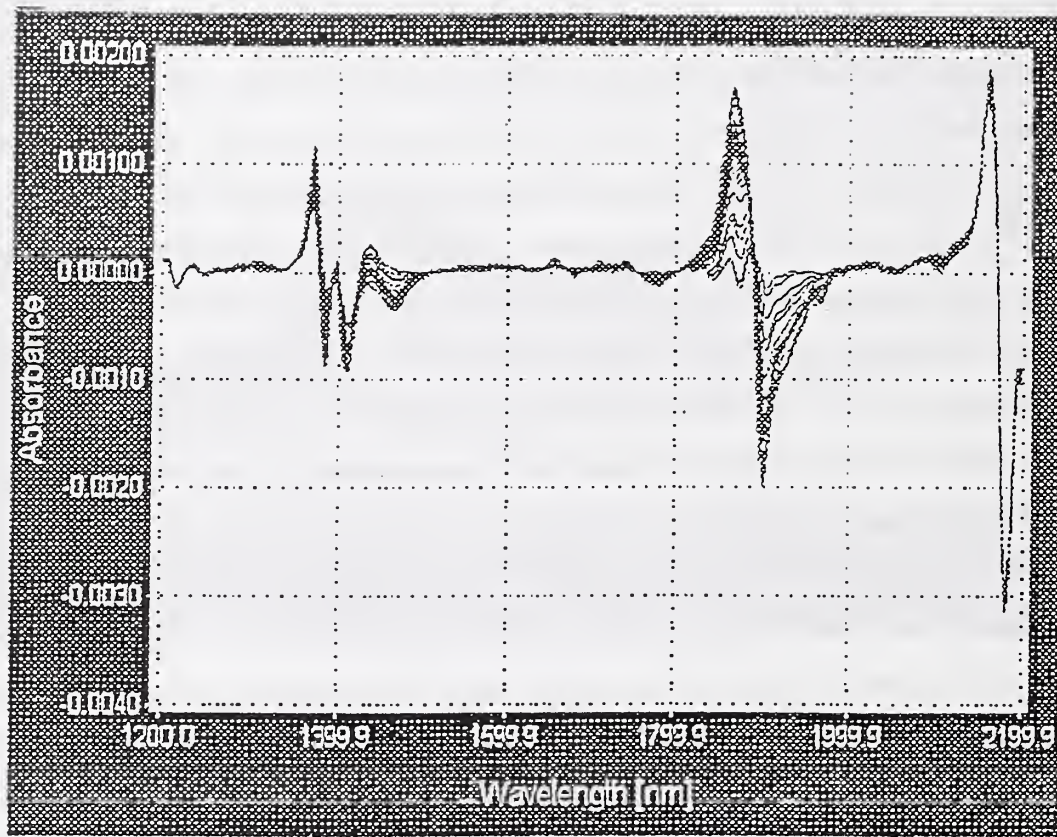


Fig. 12. The 2nd derivatives of the absorption spectra shown in Figure 11. The complex structure indicates some interaction occurred in the slurry during drying. (Data supplied by Brimose Corporation of America and General Motors Corporation).

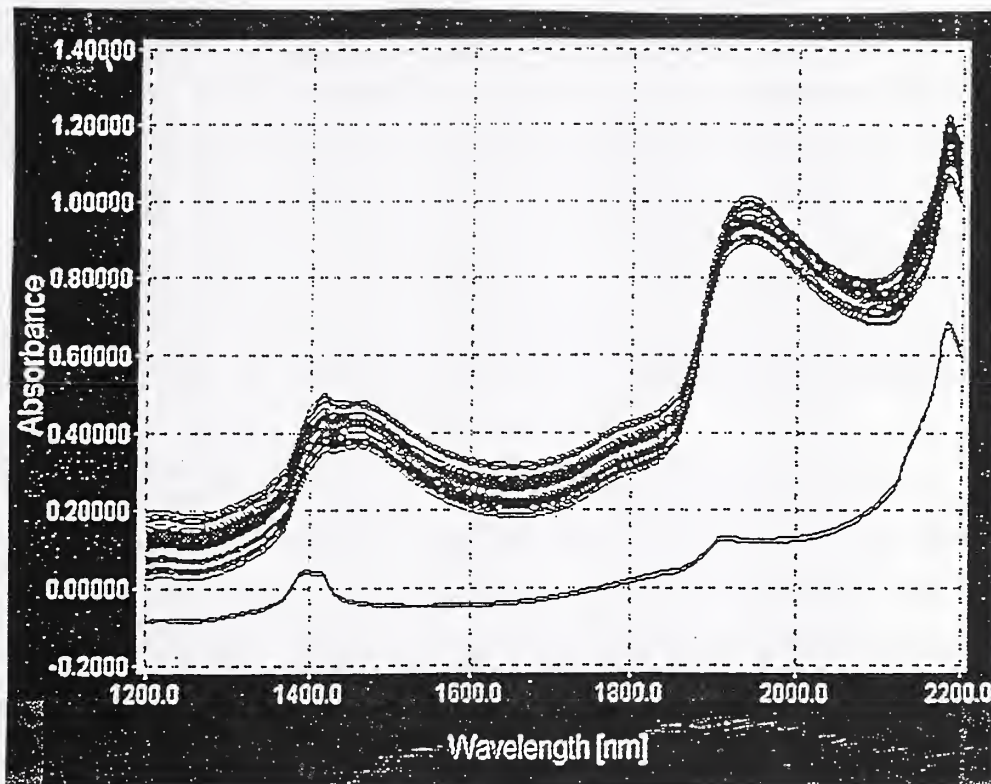


Fig. 13. A set of NIR spectra from a dry clay powder and its green bodies containing ~14% to ~31% mass fraction water. The strong ~1400 nm signal from the dry powder is due to $\text{Al}(\text{OH})_3$ which is a component of clay. (Data supplied by Brimose Corporation of America and General Motors Corporation).

Sample # :	1		2		3	
$m_{\text{dry},g}^a$:	16.056		13.771		14.792	
<u>Reading #</u>	<u>$m_{\text{total},g}^b$</u>	<u>$w_{\text{water},\%}^c$</u>	<u>$m_{\text{total},g}$</u>	<u>$w_{\text{water},\%}$</u>	<u>$m_{\text{total},g}$</u>	<u>$w_{\text{water},\%}$</u>
1	22.851	29.74	19.835	30.57	21.611	31.55
2	22.706	29.29	19.704	30.11	21.532	31.30
3	22.496	28.63	19.568	29.63	21.396	30.87
4	22.215	27.72	19.353	28.84	21.048	29.72
5	21.752	26.18	18.959	27.37	20.782	28.82
6	21.137	24.04	18.428	25.27	20.241	26.92
7	20.848	22.98	18.168	24.20	19.907	25.69
8	20.568	21.94	17.861	22.90	19.529	24.26
9	20.305	20.93	17.520	21.40	19.106	22.58
10	20.095	20.10	17.259	20.21	18.783	21.26
11	19.810	18.95	17.005	19.02	18.532	20.18
12	19.643	18.26	16.854	18.29	18.367	19.46
13	19.561	17.92	16.778	17.92	18.284	19.10
14	19.486	17.60	16.715	17.62	18.217	18.80
15	19.414	17.29	16.636	17.22	18.120	17.37
16	19.326	16.92	16.543	16.76	18.029	17.95
17	19.197	16.36	16.427	16.17	17.893	17.33
18	19.075	15.83	16.331	15.68	17.770	16.76
19	18.975	15.83	16.251	15.26	17.711	16.48
20	18.872	14.92	16.155	14.76	17.618	16.04
21	16.056	0.00	13.771	0.00	14.792	0.00

Table 2 Moisture data for three clay samples during drying as measured by NIR.

a: dry powder mass.

b: total mass (powder+water).

c: mass fraction of water = $(m_{\text{total}} - m_{\text{dry}}) / m_{\text{total}}$.

Uncertainty: $\pm 0.001g$; $\pm 0.01\%$.

and validation significantly. It should be noted that usually experiments like this tend to give excellent results, and normally results from actual parts in production tend to be less "cooperative". However, the potential shown here can be realized in actual production, if a sufficiently complete data base is used, and if during the calibration, extra care is taken to provide good reference laboratory values. A plot of measured moisture content vs. predicted moisture content from the NIR intensities is shown in Figure 14(a) for these green clay samples. A very linear plot can be obtained. On the other hand, such a plot for the slurries containing water from ~43 % to ~60 % mass fraction shows a larger uncertainty, as can be observed from Figure 14(b). Therefore, there is a limit of moisture content for which NIR measurement can provide an accurate result. Fig.14(b) is same type of plot after regression for the data in Fig. 11, for the water content ranging from 43 % to 62 % mass fraction.

One type of spectrometer was designed to be wireless and portable. It is particularly convenient for measuring moisture contents at different parts of a large, shaped green ceramic article. When the object to be measured cannot be moved because of its large size or complex, delicate shape, the sensor must change its position and orientation. Figure 15 shows the scheme that we have used for a portable NIR sensor to measure the moisture content along a production line at various stages. Stages 1 through 3 compare moisture at different points at the beginning of production – mixing, milling and “pugging”. Other stages check the moisture on various parts of green products that are critical to the products. For example, it is important that the moisture contents on the contact surface of a cup (#5) and the handle bar (#7) be as close to each other as possible to make a strong joint of the two parts. This portable sensor can even be used to check the dryer efficiency, by comparing the moisture changes before and after drying, for specimens positioned at different portions of the dryer.

This portable unit was also used to measure the moisture content of powders spread on 5 cm diameter glass dishes. The data from such measurements are plotted in Fig.16 for aluminum nitride. Results for aluminum oxide, silicon nitride, and zirconia (with

Fig. 14(a)

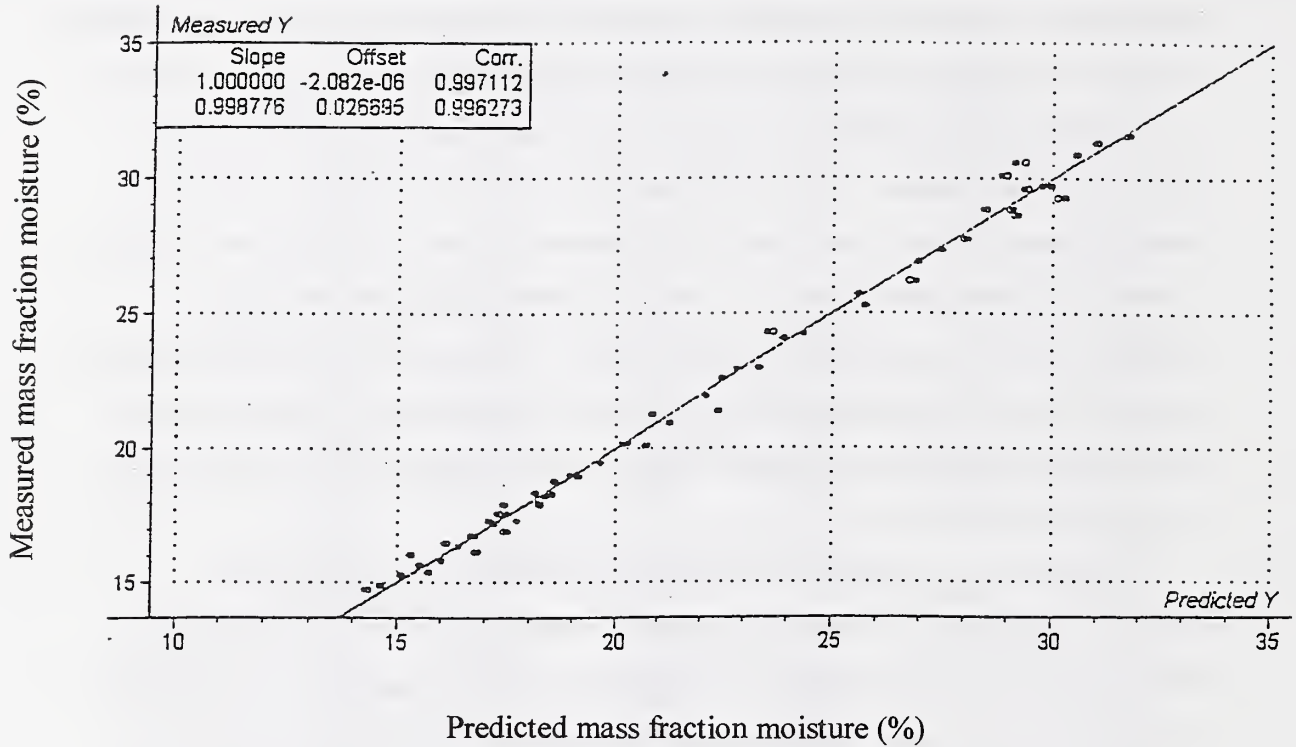


Fig. 14. Plots of measured moisture contents (by weight loss) vs. predicted moisture contents (by NIR intensities at 1460 nm) for (a) clay samples with 14 % to 32 % mass fraction water; (b) slurry samples with 43 % to 62 % mass fraction water. Both sets of data have shown a good linear relationship, however, the uncertainty is higher in the high water-containing slurries. (Data supplied by Brimrose Corporation of America and General Motors Corporation and Pfaltzgraff China).

Fig. 14(b)

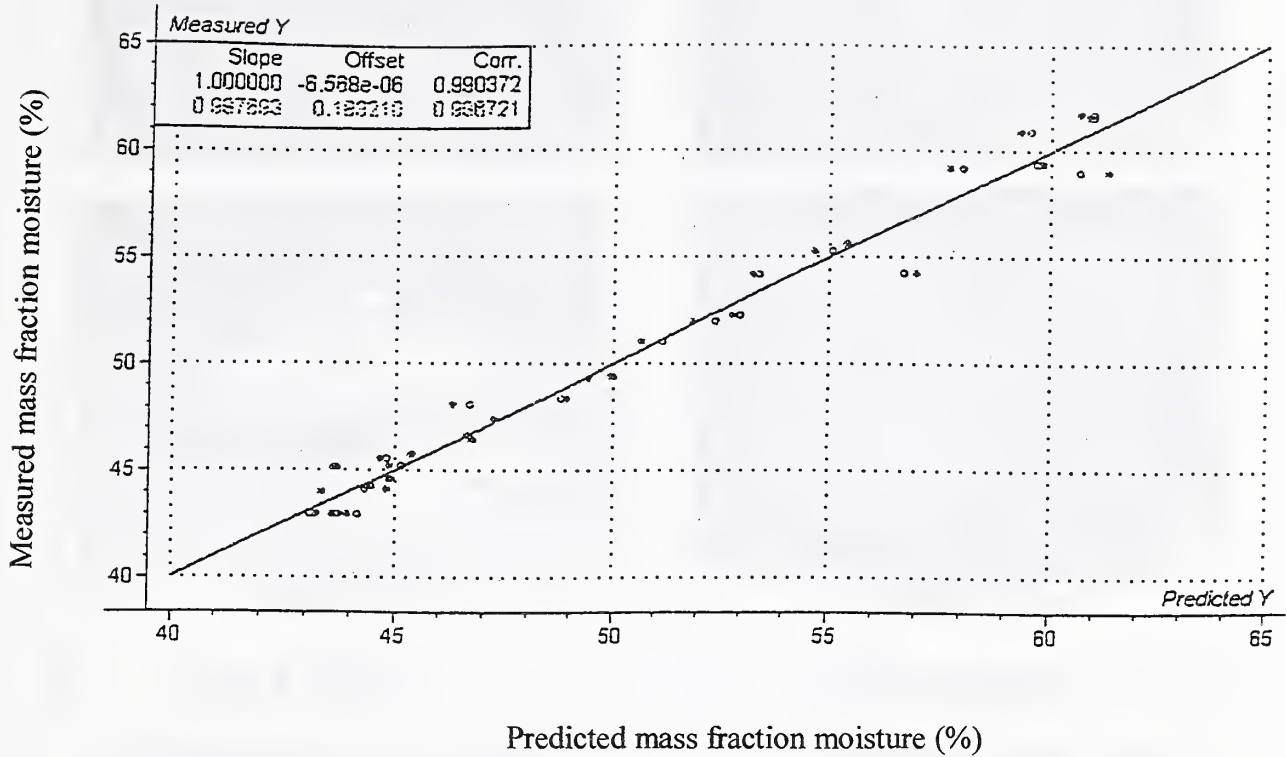
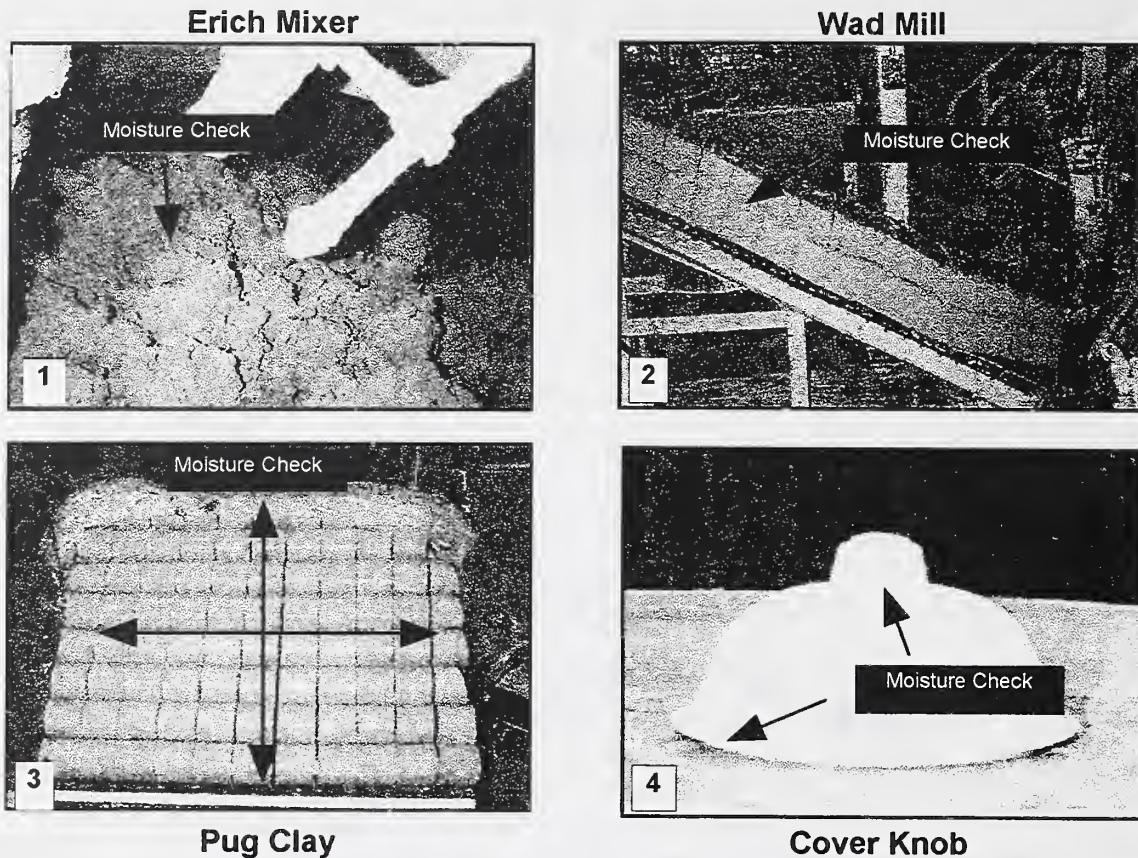


Fig. 14. Plots of measured moisture contents (by weight loss) vs. predicted moisture contents (by NIR intensities at 1460 nm) for (a) clay samples with 14 % to 32 % mass fraction water; (b) slurry samples with 43 % to 62 % mass fraction water. Both sets of data have shown a good linear relationship, however, the uncertainty is higher in the high water-containing slurries. (Data supplied by Brimrose Corporation of America and General Motors Corporation and Pfaltzgraff China).



1. **Erich Mixer**

Moisture samples are taken at the mixer after the batching/mixing process has been completed prior to moving the clay to the wad mill. Any necessary adjustments to the clay should be made at this point.

Moisture range 17.0% - 20%

2. **Wad Mill**

Moisture samples may be taken from the wad mill prior to entering the pug mill for extrusion.

Moisture range 17.0% - 20%

3. **Pug Clay**

Moisture checks are taken after the pug mill prior to the forming process. With the diversity of products currently being produced it is important to maintain the clay at the correct moistures across the clay table and from one table of clay to another.

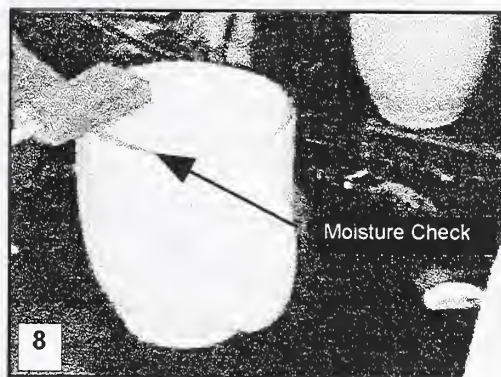
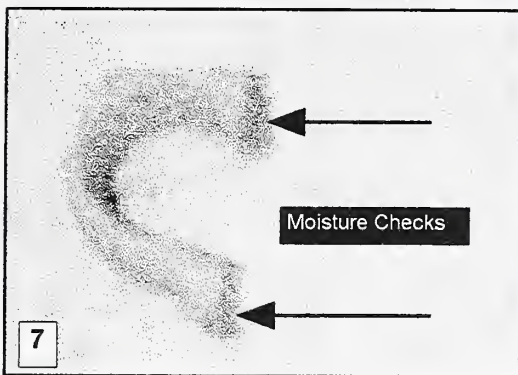
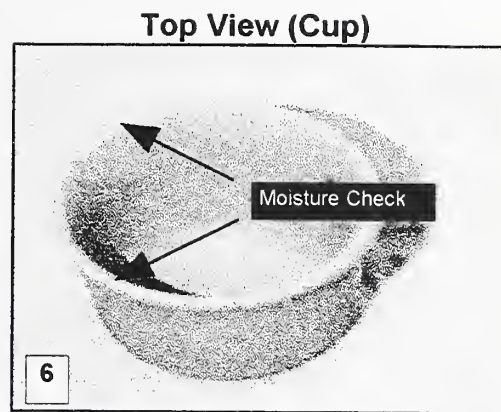
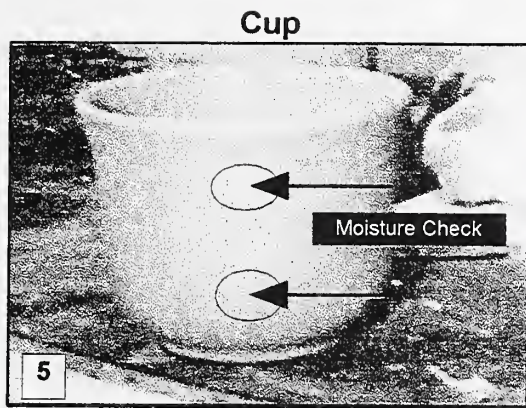
Moisture range 17.0% - 20%

4. **Covers (Lids)**

After the forming and leather hard drying process the covers are cut to form a knob on top. It is important to maintain a consistent moisture content to minimize production problems.

Moisture range 9.0% - 12%

Fig. 15. Schematics of moisture content measurements by a portable NIR sensor along a production line. A portable unit is particularly valuable for measuring a large, complex-shaped green body. (Designed by Pfaltzgraff China).



5. **Cup**

Moisture checks are taken at the handle pad location area. It is important to maintain a predetermined moisture content at this area to ensure a proper handle attachment.

Moisture range 15.0% - 18.0%

6. **Top View (Cup)**

Rim moisture is very important when force drying or applying bands on the top of the cup.

Moisture range 0% - 3%

7. **Handle**

Handle moistures are taken from the cut end of the handle. It is very important to maintain a predetermine moisture content to allow a strong bond between the cup and the handle.

Moisture range 15.0% - 18%

8. **Hand Decorating**

Moisture plays an important part in hand or machine decorating where color and ink laydown are important in maintaining a specific color or look.

Moisture range 0% - 4%

Fig. 15. Schematics of moisture content measurements by a portable NIR sensor along a production line. A portable unit is particularly valuable for measuring a large, complex-shaped green body. (Designed by Pfaltzgraff China).

Fig. 16(a)

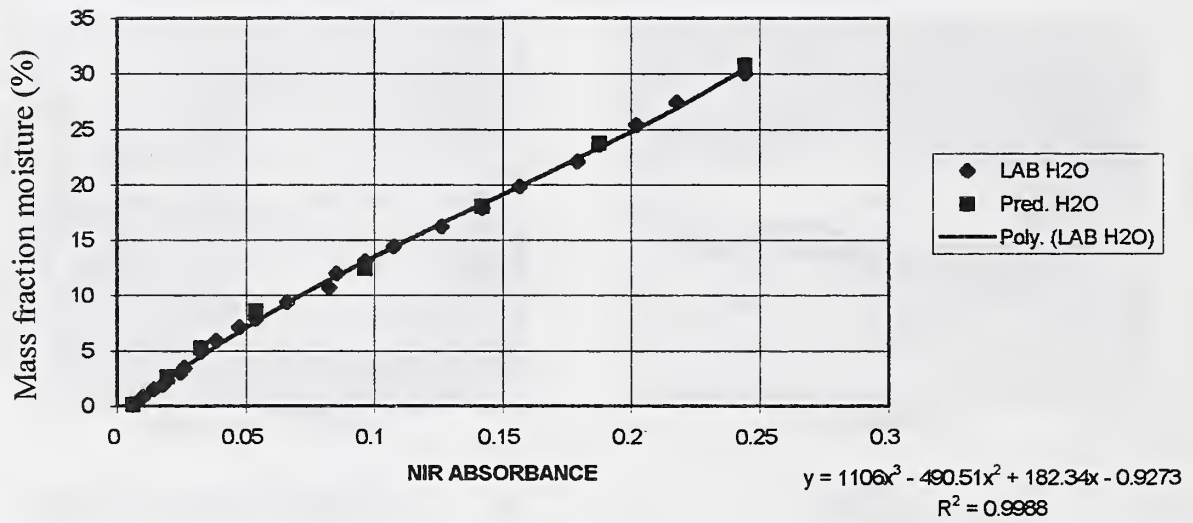


Fig. 16. Plots of mass fraction moisture vs. NIR absorbance by a portable sensor for alumina nitride powder: (a) 3rd, (b) 2nd, (c) 1st order fit, respectively. (Data from Zeltex Inc. and Pfaltzgraff China).

Fig. 16(b)

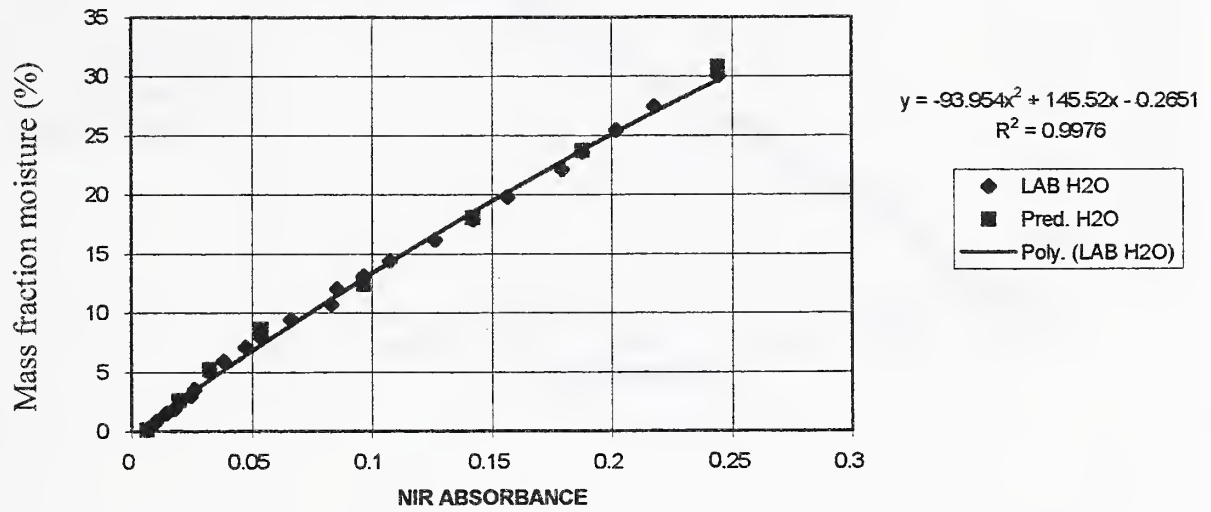


Fig. 16. Plots of mass fraction moisture vs. NIR absorbance by a portable sensor for alumina nitride powder: (a) 3rd, (b) 2nd, (c) 1st order fit, respectively. (Data from Zeltex Inc. and Pfaltzgraff China).

Fig. 16(c)

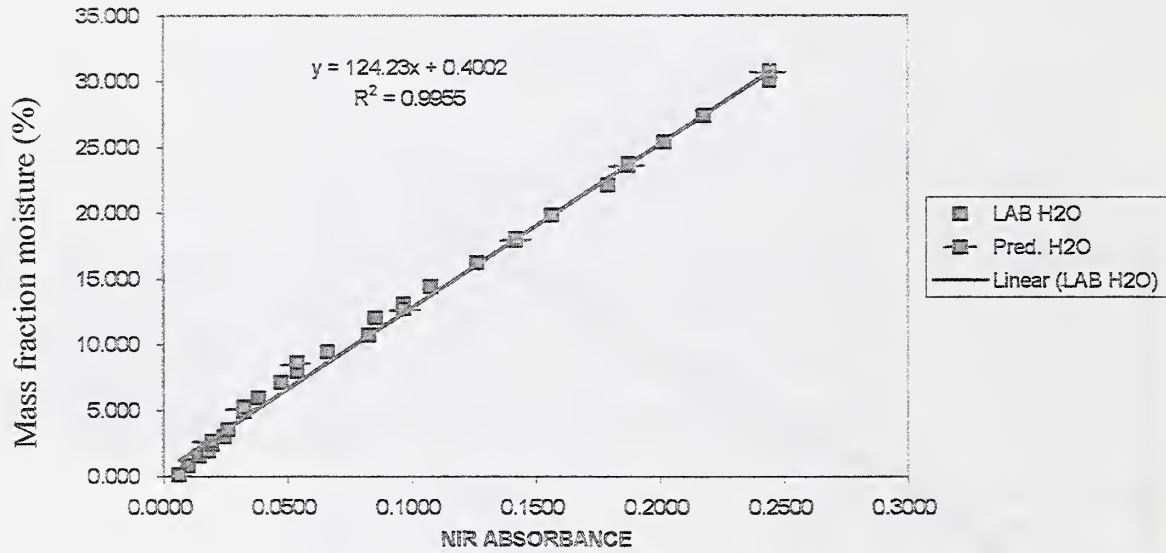


Fig. 16. Plots of mass fraction moisture vs. NIR absorbance by a portable sensor for alumina nitride powder: (a) 3rd, (b) 2nd, (c) 1st order fit, respectively. (Data from Zeltex Inc. and Pfaltzgraff China).

yttria) powder are shown in Figures 17, 18, and 19 respective. Each figure shows the results for the curve fitting of 3rd, 2nd, and 1st order, respectively.

One should also bear in mind that NIR, compared to NMR and microwave techniques, still has a limit in detection penetration and still must be considered a semi-surface technique. The advantage of the NIR technique is its portability. Some of the spectrometers were designed as handheld units, a design feature that was very convenient when measuring the local moisture content in a large green body. Some NIR spectrometers use an acousto-optic filter to further stabilize the beam and improve resolution and thereby to widen the instrument capability. All of the instruments, moreover, can be installed on-line for ceramic applications.

Fig. 17(a)

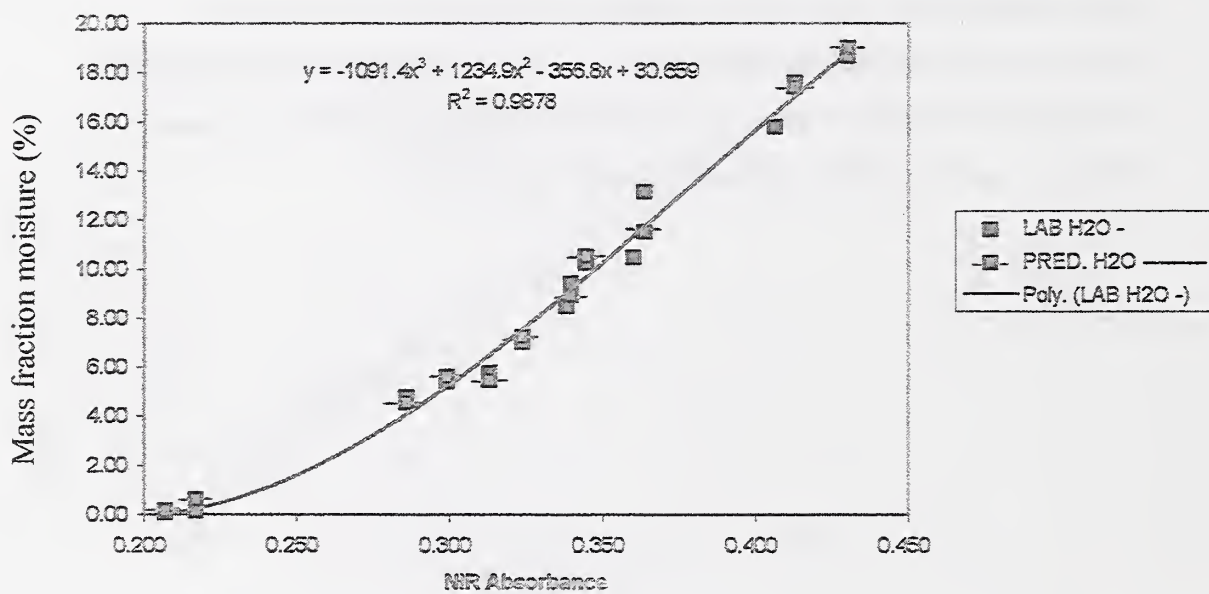


Fig. 17. Plots of mass fraction moisture vs. NIR absorbance by a portable sensor for alumina oxide powder: (a) 3rd, (b) 2nd, (c) 1st order fit, respectively. (Data from Zeltex Inc. and Pfaltzgraff China).

Fig. 17(b)

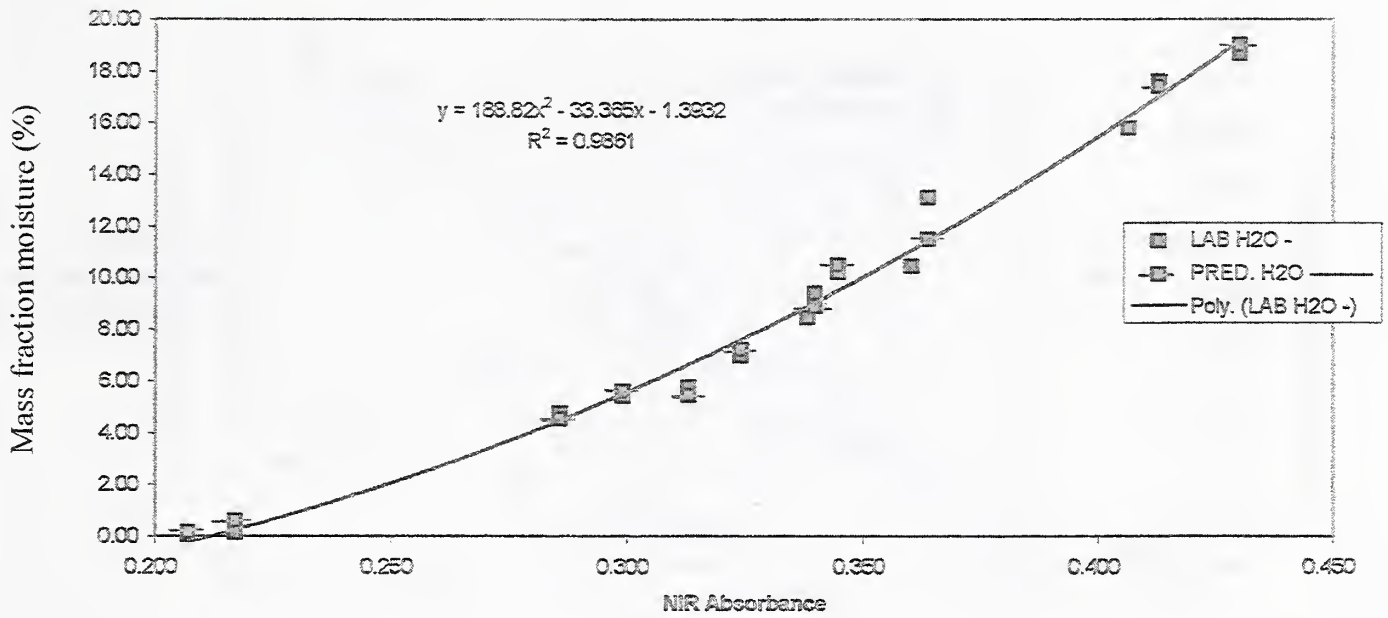


Fig. 17. Plots of mass fraction moisture vs. NIR absorbance by a portable sensor for alumina oxide powder: (a) 3rd, (b) 2nd, (c) 1st order fit, respectively. (Data from Zeltex Inc. and Pfaltzgraff China).

Fig. 17(c)

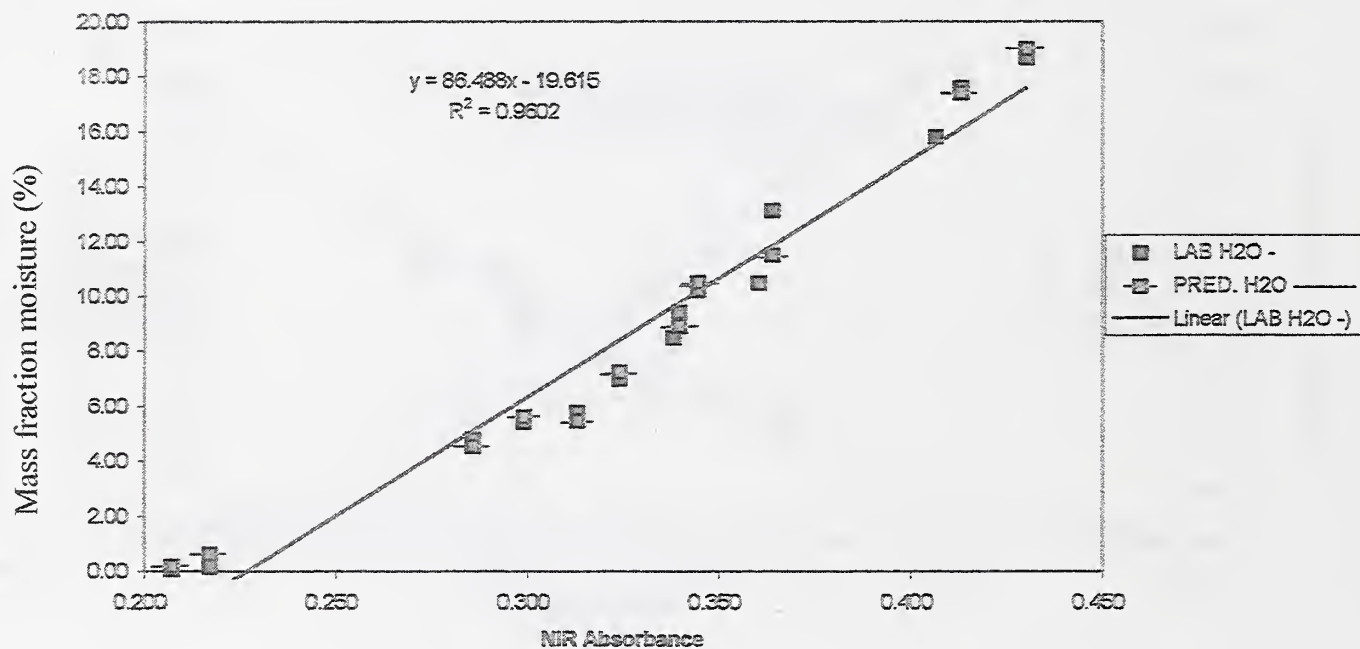


Fig. 17. Plots of mass fraction moisture vs. NIR absorbance by a portable sensor for alumina oxide powder: (a) 3rd, (b) 2nd, (c) 1st order fit, respectively. (Data from Zeltex Inc. and Pfaltzgraff China).

Fig. 18(a)

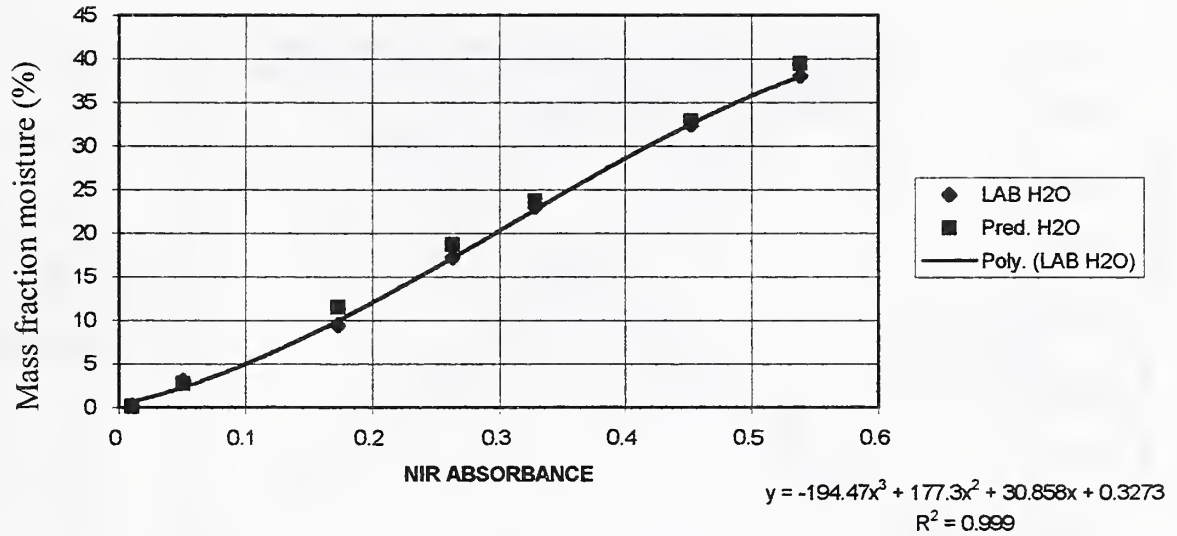


Fig. 18. Plots of mass fraction moisture vs. NIR absorbance by a portable sensor for silicon nitride powder: (a) 3rd, (b) 2nd, (c) 1st order fit, respectively. (Data from Zeltex Inc. and Pfaltzgraff China).

Fig. 18(b)

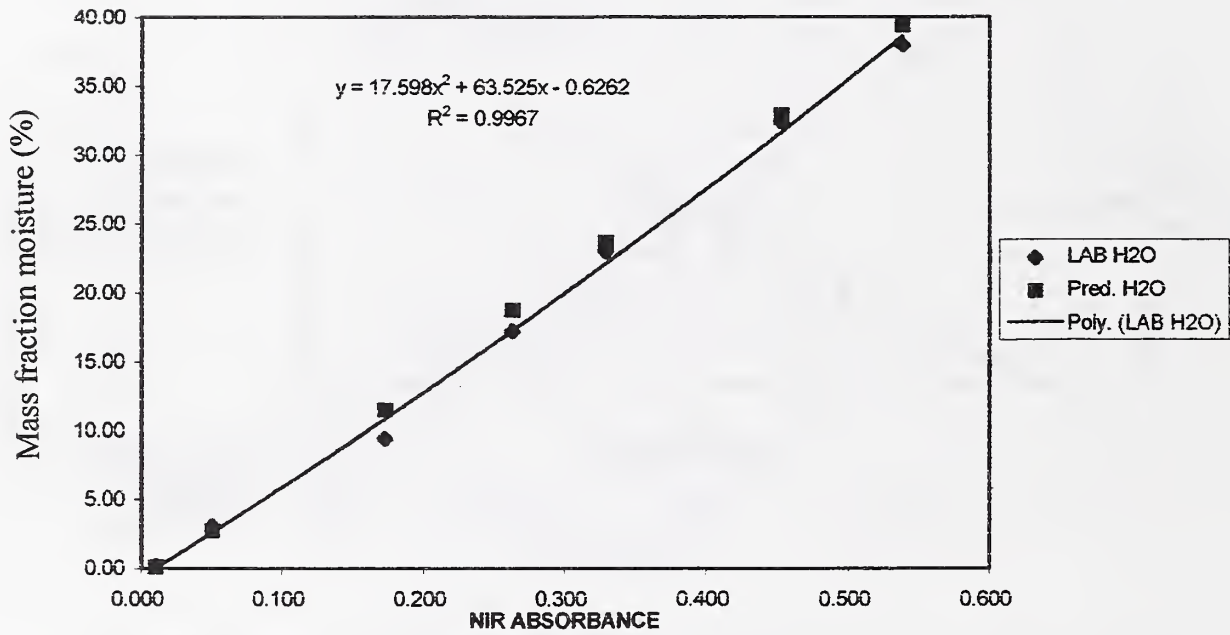


Fig. 18. Plots of mass fraction moisture vs. NIR absorbance by a portable sensor for silicon nitride powder: (a) 3rd, (b) 2nd, (c) 1st order fit, respectively. (Data from Zeltex Inc. and Pfaltzgraff China).

Fig. 18(c)

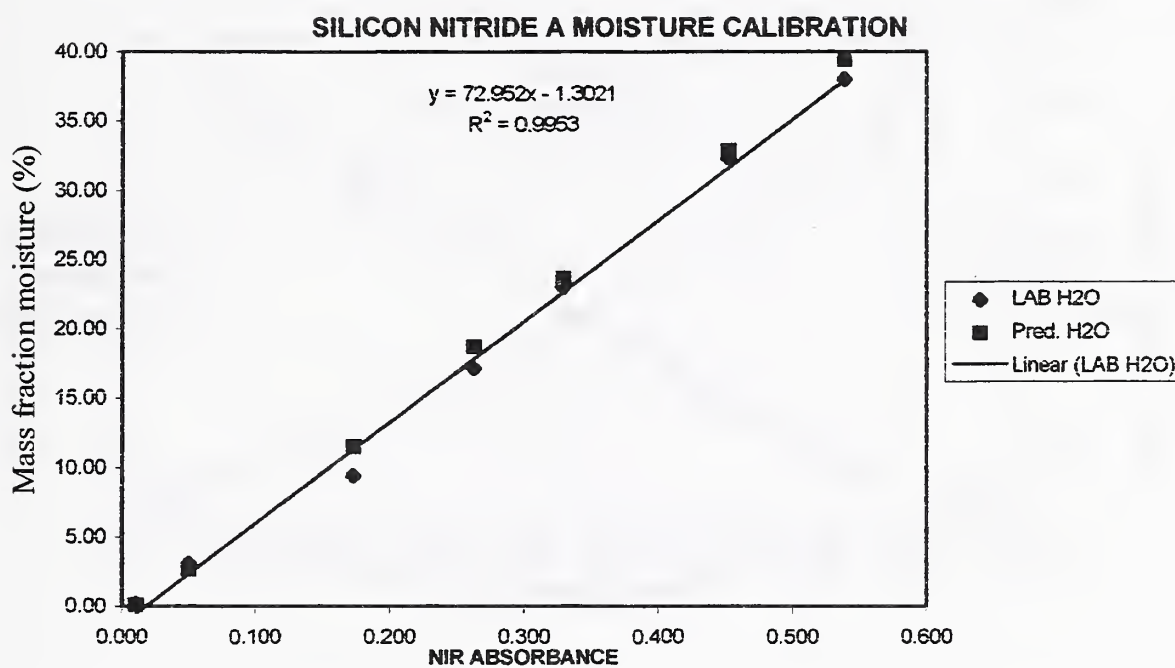


Fig. 18. Plots of mass fraction moisture vs. NIR absorbance by a portable sensor for silicon nitride powder: (a) 3rd, (b) 2nd, (c) 1st order fit, respectively. (Data from Zeltex Inc. and Pfaltzgraff China).

Fig. 19(a)

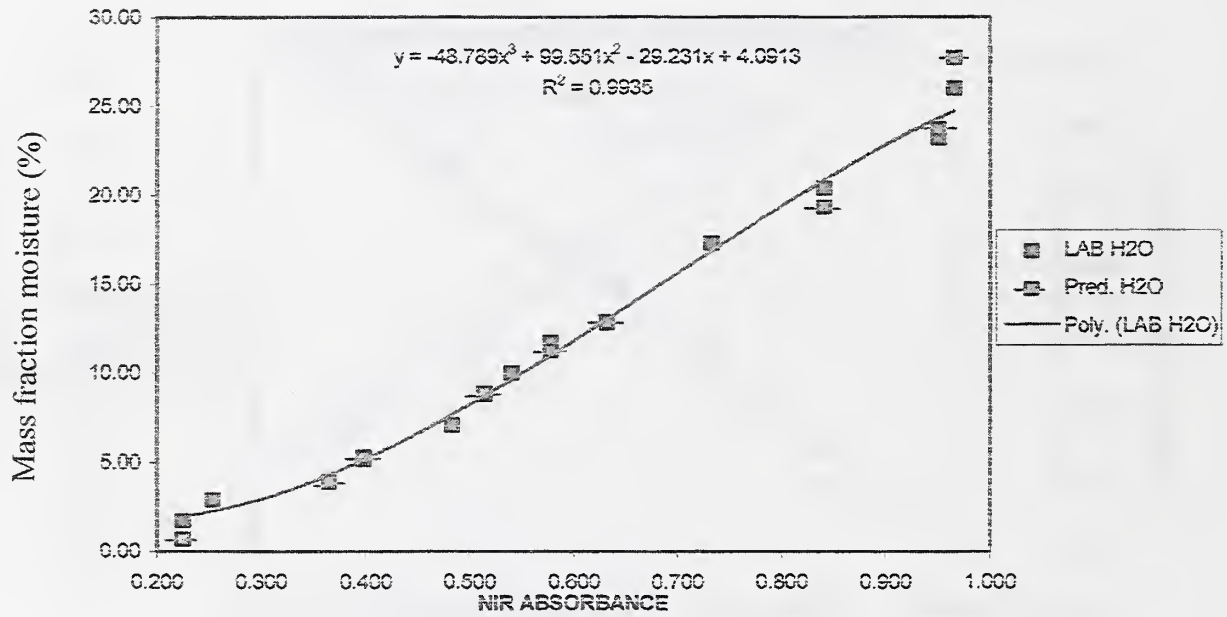


Fig. 19. Plots of mass fraction moisture vs. NIR absorbance by a portable sensor for zirconia (containing yttria) powder: (a) 3rd, (b) 2nd, (c) 1st order fit, respectively. (Data from Zeltex Inc. and Pfaltzgraff China).

Fig. 19(b)

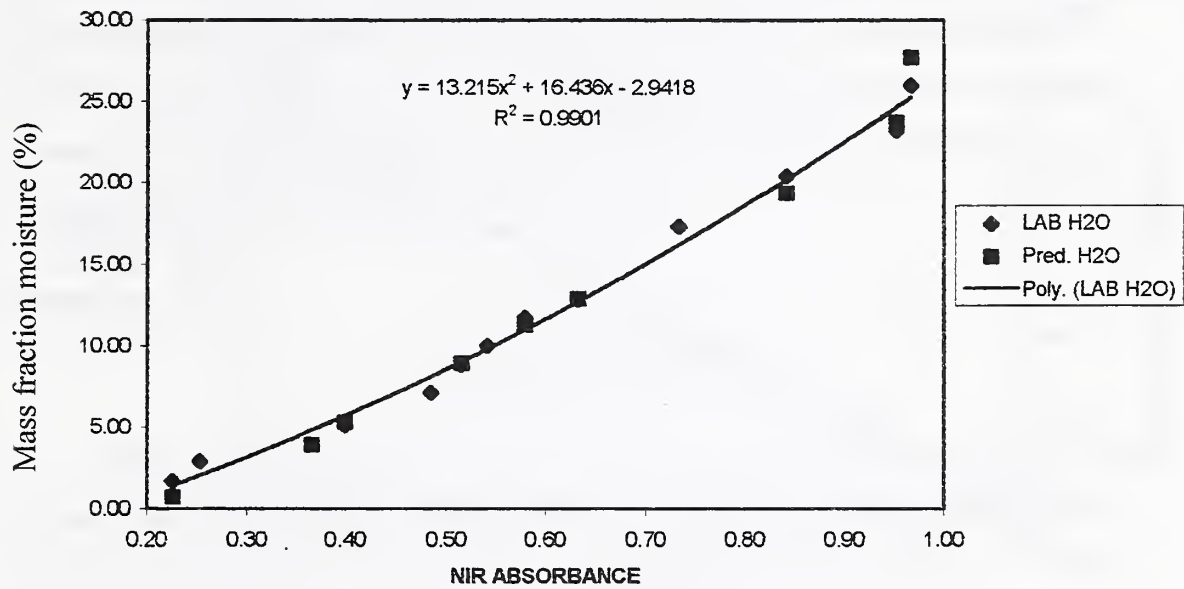


Fig. 19. Plots of mass fraction moisture vs. NIR absorbance by a portable sensor for zirconia (containing yttria) powder: (a) 3rd, (b) 2nd, (c) 1st order fit, respectively. (Data from Zeltex Inc. and Pfaltzgraff China).

Fig. 19(c)

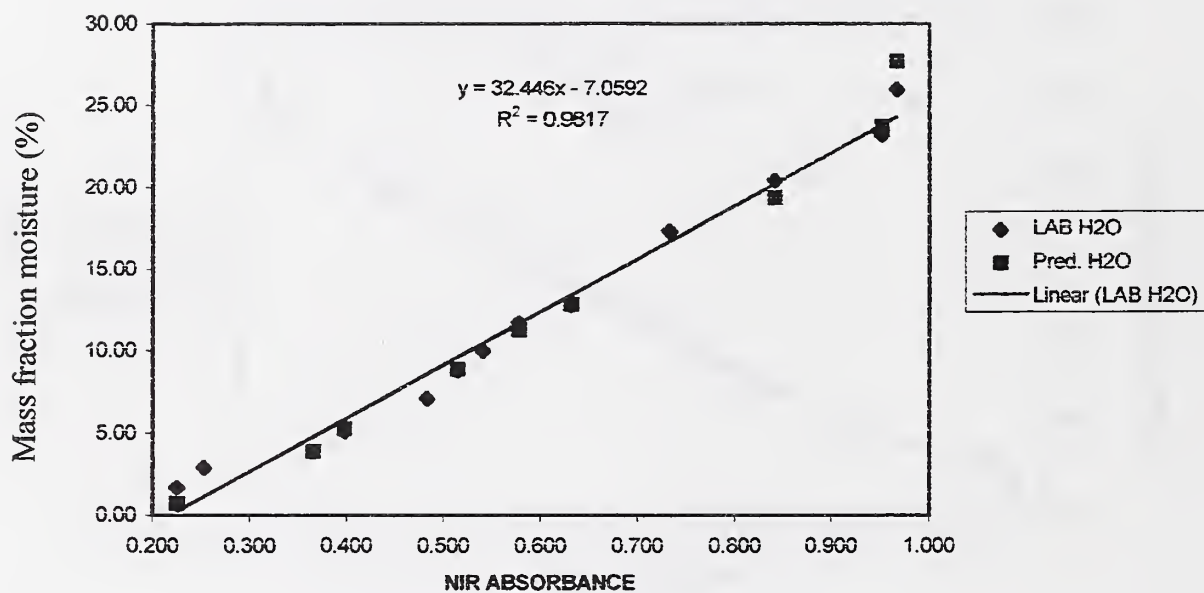


Fig. 19. Plots of mass fraction moisture vs. NIR absorbance by a portable sensor for zirconia (containing yttria) powder: (a) 3rd, (b) 2nd, (c) 1st order fit, respectively. (Data from Zeltex Inc. and Pfaltzgraff China).

3. CONCLUSIONS

Moisture control during ceramic processing is critical for product quality improvement and cost reduction. Various moisture measurement techniques developed for other industries were reviewed, and some of them were found to be applicable for ceramic processing. The gravimetric method is still considered to be the primary technique for calibration of other techniques. Near infrared and microwave methods are both promising due to the low cost and ease of operation. Each technique has its strengths and limitations; and both can be installed on-line or off-line. The emerging NMR and NMR imaging techniques can provide additional information on the physical state of water and its spatial distribution in ceramics. A comparison of the advantages and the limitations of these techniques is shown in Table 3.

ACKNOWLEDGEMENTS

The work presented in this report is a collective effort of members of the Moisture Measurement Team under Ceramic Processing Consortium. The authors would like to express their gratitude for contributions from all team members in manpower, samples, equipment time, and technical expertise to make the work possible.

Technique	Advantages	Limitations
Weight loss	low cost, simple, accurate	destructive, cannot be on-line
Microwave	low cost, simple, bulk technique off- and on-line , nondestructive	inaccurate for samples with dielectric constant comparable to water
NMR and MRI	bulk techniques, give information on chemical and physical state, distribution of water molecules, nondestructive	high cost, complex, currently off-line
NIR	low cost, simple, nondestructive, on- and off-line	limited penetration, sensitive to sample color

Table 3. A comparison of advantages and limitations of moisture measurement techniques for ceramic processing

REFERENCES

- [1]. J. Mitchell, Jr., and D. M. Smith, "Aquametry", P. J. Elving, J. D. Winefordner, I. M. Kolthoff, Eds., John Wiley & Sons, New York, 1980.
- [2]. A. Pande, "Handbook of Moisture Determination and Control", Marcel Dekker, Inc., New York, 1974.
- [3]. K. Fischer, *Z. Angew. Chem.* Vol. 48, 394 (1935).
- [4]. "Spectroscopy and Molecular Structure", Chapter 10, G. W. King, Holt, Rinehart and Winston, Inc., New York, 1965.
- [5]. "Metal Ions in Aqueous Solution", chapter 3, J. P. Hunt, W. A. Benjamin, Inc., New York, 1965.
- [6]. R. J. King, "Microwave Sensors For Process Control, Part I: Transmission Sensors", *SENSORS*, page 68-79, Sept. (1992).
- [7]. R. J. King, "Microwave Sensors For Process Control, Part II: Open Resonator Sensors", *SENSORS*, Page 25-29, Oct. (1992).
- [8]. R. J. King, "On-Line Industrial Applications of Microwave Moisture Sensors", in *SENSORS UPDATE*, vol. 7, H. Baltes, W. Gopel and J. Hesse, Eds. Wiley-VCH, 2000 (in press).
- [9]. M. Werner and R. King, "Microwave Sensors for Imaging Moisture and Flaws in Advanced Composites", *Review of Progress in Quantitative Nondestructive Evaluation*, vol. 15, 1995, page 1 – 7, Plenum Publishing Corporation, NY, NY.

- [10]. L. Pauling, "Hydrogen Bonding", D. Hadzi, Ed., Pergamon Press, New York, 1951.
- [11]. C. P. Slichter "Principles of Magnetic Resonance", 3rd Edit., Chapter 1, Springer-Verlag, New York, New York, 1989.
- [12]. P. S. Wang, S. G. Malghan, S. J. Dapkunas, K. F. Hans, and R. Raman, "NMR Characterization of Injection Moulded Alumina Green Compacts, Part I: Nuclear Spin-Spin Relaxation", J. Mat. Sci. **30**, 1059-1064 (1995).
- [13]. P. S. Wang, S. G. Malghan, S. J. Dapkunas, K. F. Hans, and R. Raman, "NMR Characterization of Injection Moulded Alumina Green Compacts, Part II: T_2 -Weighted Proton Imaging", J. Mat. Sci. **30**, 1069-1074 (1995).
- [14]. P. S. Wang, "NMR Characterization of Silicon Nitride: Slurry Homogeneity by T_2 -Weighted Proton Imaging", J. Mat. Sci. **32**, 5697-5702 (1996).
- [15]. P. S. Wang, D. B. Minor, and S. G. Malghan, "Binder Distribution in Si_3N_4 Ceramic Green Bodies Studied by Stray-Field NMR Imaging", J. Mat. Sci. **28**, 4940-4943 (1993).
- [16]. "Molecular Vibrations", Chapter 1, E. B. Wilson, Jr., J. C. Decius, and P. C. Cross, McGraw-Hill Book Company, Inc., New York, 1955.
- [17]. T. N. Wittberg and P. S. Wang, "XPS Study of the Dehydration of Clay and Kaolin Powders", Surface and Interface Analysis **27**, 936-940 (1999).

LIST OF FIGURES

- Fig. 1. TGA profile of a stoneware clay sample containing 14 % mass fraction water heated at 105 °C. Note that the profile shows two different drying rates.....7
- Fig. 2. The design of a two-way transmission microwave system for moisture measurement. (Reproduced with permission from R. J. King of KDC Technology).....10
- Fig. 3. Typical applications of microwave resonator moisture sensors (Reproduced with permission from R. J. King of KDC Technology).....13
- Fig. 4. Nuclear energy levels of a proton in an external magnetic field. There are two relaxation mechanisms, nuclear spin-spin or nuclear spin-crystal lattice, when it returns from the excited state to ground state.....16
- Fig. 5. A block diagram of a NMR spectrometer with imaging capability. The gradient coil is used to convert a spectroscopic signal to a spatially resolved picture.....17
- Fig. 6. NMR lineshapes of a clay sample containing, from top to bottom, unheated sample with crack, unheated without crack, heated at 105 °C for 24 min., heated at 105 °C for 39 min, and after 63 min heating, all moisture was removed and the broad line is due to $\text{Al}(\text{OH})_3$. Note that “free water” accumulated in the crack and has a much narrower linewidth because of molecular tumbling (top curve)...20
- Fig. 7. Nuclear spin-echo intensity decay of moisture from an Alumina sample. The fast decay region represents bound water (14.2 %) while the slow decay region is due to free water (16.8 %). (Data from Bruker Minispec).....22

- Fig. 8. A slice from a 3D NMR image, showing internal defect points detected in a green ceramic sample. The spots with high intensity will be weak points after firing.....25
- Fig. 9. Molecular vibration modes of a water molecules. They are, from left to right, symmetric stretching, “scissoring”, and asymmetric stretching, respectively.....26
- Fig. 10. A block diagram of an IR (or NIR) spectrometer. The difference between the two lies in the frequency region of detection. NIR penetrates deeper into the sample. (Reproduced from Zeltex’s literature with permission).....27
- Fig. 11. A sequence of water NIR spectra from a slurry containing ~60 % mass fraction of water during drying. The peak at ~1460 nm (~7300 cm^{-1}) is the first overtone of 3652 cm^{-1} (O-H symmetric stretching from water molecules). The ~1940 nm (~5250 cm^{-1}) peak is from the combination of 3652 cm^{-1} and 1595 cm^{-1} “scissoring”. Note the weak ~1400 nm peak remains even when the sample is dry. (Data supplied by Brimrose Corporation of America and General Motors Corporation).....32
- Fig. 12. The 2nd derivatives of the absorption spectra shown in Figure 11. The complex structure indicates some interaction occurred in the slurry during drying. (Data supplied by Brimrose Corporation of America and General Motors Corporation).....34
- Fig. 13. A set of NIR spectra from a dry clay powder and its green bodies containing ~14% to ~31% mass fraction water. The strong ~1400 nm signal from the dry powder is due to $\text{Al}(\text{OH})_3$, which is a component of clay. (Data supplied by Brimrose Corporation of America and General Motors Corporation).....35

- Fig. 14. Plots of measured moisture contents (by weight loss) vs. predicted moisture contents (by NIR intensities at 1460 nm) for (a) clay samples with 14 % to 32 % mass fraction water; (b) slurry samples with 43 % to 62 % mass fraction water. Both sets of data have shown a good linear relationship, however, the uncertainty is higher in the high water-containing slurries. (Data supplied by Brimrose Corporation of America and General Motors Corporation and Pfaltzgraff China).....38-39
- Fig. 15. Schematics of moisture content measurements by a portable NIR sensor along a production line. A portable unit is particularly valuable for measuring a large, complex-shaped green body. (Designed by Pfaltzgraff China).....40-41
- Fig. 16. Plots of mass fraction moisture vs. NIR absorbance by a portable sensor for alumina nitride powder: (a) 3rd, (b) 2nd, (c) 1st order fit, respectively. (Data from Zeltex Inc. and Pfaltzgraff China).....42-44
- Fig. 17. Plots of mass fraction moisture vs. NIR absorbance by a portable sensor for alumina oxide powder: (a) 3rd, (b) 2nd, (c) 1st order fit, respectively. (Data from Zeltex Inc. and Pfaltzgraff China).....46-48
- Fig. 18. Plots of mass fraction moisture vs. NIR absorbance by a portable sensor for silicon nitride powder: (a) 3rd, (b) 2nd, (c) 1st order fit, respectively. (Data from Zeltex Inc. and Pfaltzgraff China).....49-51
- Fig. 19. Plots of mass fraction moisture vs. NIR absorbance by a portable sensor for zirconia (containing yttria) powder: (a) 3rd, (b) 2nd, (c) 1st order fit, respectively. (Data from Zeltex Inc. and Pfaltzgraff China).....52-54

LIST OF TABLES

Table 1	Mass fraction of solids as a function of drying time in air, based on weighing samples of the coating on a foamed polystyrene sample.....	31
Table 2	Moisture data for three clay samples during drying as measured by NIR.....	36
Table 3	A comparison of the advantages and limitations of moisture measurement Techniques for ceramic processing.....	56

